Reggeon calculus for the production amplitude. II

Jochen Bartels*
Fermi National Accelerator Laboratory, Batavia, Illinois 60510†
(Received 25 November 1974)

A Reggeon calculus for the production amplitude is derived by using Gribov's method of analyzing hybrid Feynman diagrams. We find that, for any Reggeon diagram, the production amplitude can be written in the representation discussed in part I of this study, and each term can be evaluated according to rules which are a rather straightforward extension of Gribov's Reggeon calculus and have the same character of a nonrelativistic field theory. We briefly show how the concept of Reggeon field theory can be applied to production amplitudes.

I. INTRODUCTION

In the first part of our study[1] (henceforth referred to as paper I) we derived and discussed in some detail a representation of the $2 \to n$ production amplitude in the multi-Regge limit. In this representation, the amplitude is written as a sum of terms, each of which corresponds to a certain set of simultaneous singularities. Signature factors are shown explicitly, and the remaining coefficient functions are real. For the $2 \to 3$ amplitude (Fig. 1)

$$T_{2\to3} = g(t_1)g(t_2)[\, s^{\alpha_1} s_{bc}{}^{\alpha_2-\alpha_1} \xi_{\alpha_1} \xi_{\alpha_2\alpha_1} V_L(\eta) + s^{\alpha_2} s_{ab}{}^{\alpha_1-\alpha_2} \xi_{\alpha_2} \xi_{\alpha_1\alpha_2} V_R(\eta)\,] \,, \tag{1.1}$$

where $g(t)$ and $V_{R,L}(\alpha_1\alpha_2 t_1 t_2 \eta)$ are real (analytic) functions for the Reggeon–two-particle vertex and two-Reggeon–particle vertex, respectively.

This discussion had been based entirely on amplitudes with pure Regge-pole exchange. In this second part we want to extend our consideration to amplitudes which contain Regge cuts as well, and it will turn out that the representation (1.1) is just the right one to be used. When we write it as a double Sommerfeld-Watson transform,

$$T_{2\to3} = \left(-\frac{1}{4i}\right)^2 \times \int dj_1 dj_2 [\, s^{j_1} s_{bc}{}^{j_2-j_1} \xi_{j_1} \xi_{j_2 j_1} F_L(j_1 j_2 t_1 t_2 \eta) + s^{j_2} s_{ab}{}^{j_1-j_2} \xi_{j_2} \xi_{j_1 j_2} F_R(j_1 j_2 t_1 t_2 \eta)\,] \,, \tag{1.2}$$

with appropriate functions $F_{L,R}$, then we will find that this form holds for any $2 \to 3$ amplitude, including those with Regge-cut contributions, and all information about the j-plane structure is contained in the coefficient functions $F_{L,R}$, which are free from phase factors.

In examining the effect of Regge cuts in the production amplitude, we follow the pattern of Gribov's[2] work on the $2 \to 2$ amplitude, i.e., we shall study hybrid Feynman diagrams and use Sudakov techniques. As the result, we shall find that a Reggeon calculus can be formulated which is a rather straightforward extension of Gribov's rules and has the same structure as a nonrelativistic field theory. Using the representation (1.2), this Reggeon calculus provides us with rules for the calculation of Regge-cut contributions to the coefficient functions F_L and F_R. One particularly interesting aspect of this is that it will be possible to apply the concept of Reggeon field theory[3] to production processes.

In the course of deriving our Reggeon calculus, we first shall examine hybrid Feynman diagrams of the $2 \to 3$ amplitude. Then we extend our considerations to the $2 \to 4$ process, and from this we derive our general rules. In order to make the reading of the paper as convenient as possible, we shall present all our results in the final section, while calculations will be done in Secs. II and III, and an appendix. The final section will also contain a brief derivation of the Reggeon field theory which recently has been used by Migdal *et al.*[4] During our calculations in Secs. II and III we frequently refer to Gribov's paper as well as to two papers of Drummond[5] and Campbell[6] who studied some hybrid Feynman diagrams for the production amplitude.

II. REGGEON DIAGRAM TECHNIQUE FOR THE $2 \to 3$ AMPLITUDE

The simplest diagram that contributes to the double-Regge behavior of the $2 \to 3$ process is shown in Fig. 1. The momentum-transfer vectors are related to the incoming momenta and the energies s_{ab}, s_{bc}, s through

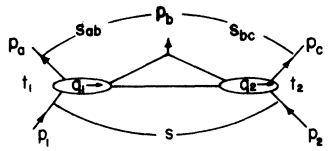

FIG. 1. The simplest diagram for the $2\to 3$ amplitude.

$$q_1 = \frac{s_{bc}-m^2}{2s}(p_1+p_2) + \frac{s_{bc}-m^2-2q_1^2}{2(s-4m^2)}(p_1-p_2)+q_{1\perp}\,,$$
$$q_2 = -\frac{s_{ab}-m^2}{2s}(p_1+p_2) + \frac{s_{ab}-m^2-2q_2^2}{2(s-4m^2)}(p_1-p_2)+q_{2\perp}\,, \tag{2.1}$$

where $q_{1\perp}$ and $q_{2\perp}$ have only components perpendicular to the incoming momenta p_1 and p_2. In the double-Regge limit

$$s, s_{ab}, s_{bc}\to\infty\,, \qquad t_1,\ t_2,\ \eta=\frac{s_{ab}s_{bc}}{s}\ \text{fixed}\,, \tag{2.2}$$

it follows from (2.1) that

$$q_{1\perp}^2\to t_1,\quad q_{2\perp}^2\to t_2 \tag{2.3}$$

and

$$\frac{s_{ab}s_{bc}}{s}=m_b^2-(q_1-q_2)_\perp^2=\eta\,. \tag{2.4}$$

Assuming for the moment that the two blobs in Fig. 1 have Regge-pole behavior with factorizing residue functions, we have for the asymptotic behavior of Fig. 1 the expression (1.1) which we now write as

$$T_{2\to 3}=g(t_1)g(t_2)s_{ab}^{\alpha_1}s_{bc}^{\alpha_2}[\eta^{-\alpha_1}V_L\xi_{\alpha_1}\xi_{\alpha_2\alpha_1}+\eta^{-\alpha_2}V_R\xi_{\alpha_2}\xi_{\alpha_1\alpha_2}]\,. \tag{2.5}$$

(2.5) can also be represented as a double Mellin transform:

$$T_{2\to 3}=\left(-\frac{1}{4i}\right)^2\int dj_1dj_2 s_{ab}^{j_1}s_{bc}^{j_2}\times[\eta^{-j_1}\xi_{j_1}\xi_{j_2j_1}F_L(j_1j_2t_1t_2\eta)+\eta^{-j_2}\xi_{j_2}\xi_{j_1j_2}F_R(j_1j_2t_1t_2\eta)]\,, \tag{2.6}$$

where

$$F_{L,R}(j_1j_2t_1t_2\eta)=\left(\frac{2}{\pi}\right)^2 g(t_1)g(t_2)G_{j_1}(t_1)\times V_{L,R}(j_1j_2t_1t_2\eta)G_{j_2}(t_2)\,, \tag{2.7}$$

$$G_j(t)=\frac{1}{j-\alpha(t)}\,. \tag{2.8}$$

Obviously, (2.6) is the same as (1.2). For simplicity in our following calculations we shall use (2.6) rather than (1.2), and one of our results will be that this form is unaffected by the presence of any cuts. All effects of cut contributions will be contained in F_L and F_R.

As the next step we consider the diagram in Fig. 2. A detailed analysis has been given in Ref. 5 and we quote only the result[7]:

$$-\frac{i\pi^2}{4}\int\frac{d^2k_\perp}{(2\pi)^2}\int\frac{dl_1dl_2dl_3}{(2\pi i)^3}s_{ab}^{l_1}s_{bc}^{l_2}s^{l_3-1}G_{l_1}((q_1-k)_\perp^2)G_{l_2}((q_2-k)_\perp^2)G_{l_3}(k_\perp^2)\xi_{l_3}N_{l_1l_3}N_{l_2l_3}\times[\eta^{-l_1}\xi_{l_1}\xi_{l_2l_1}V_L+\eta^{-l_2}\xi_{l_2}\xi_{l_1l_2}V_R]\,. \tag{2.9}$$

The N's stand for the crossed box graphs at both sides of Fig. 2 and describe the coupling of two Reggeons to two particles. They are identical to the functions which appear in the $2\to 2$ amplitude (Fig. 3). The energy factors in (2.9) can be rewritten as

$$s_{ab}^{l_1+l_3-1}s_{bc}^{l_2+l_3-1}\eta^{-(l_3-1)}\,. \tag{2.10}$$

We further combine the signature factor ξ_{l_3} with

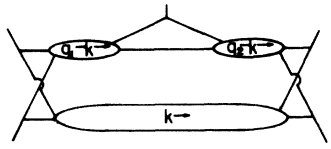

FIG. 2. A cut contribution to the $2\to 3$ amplitude.

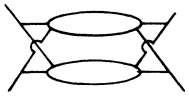

FIG. 3. Two-Reggeon cut in the $2\to 2$ amplitude.

those in the bracket. Using the identity

$$\xi_{l_1}\xi_{l_3} = \frac{e^{-i\pi(l_1+l_3-1)}+\tau_1\tau_3}{\sin\pi(l_1+l_3-1)}\, i\gamma_{l_1 l_3},$$

$$\gamma_{l_1 l_3} = \frac{\cos\{\frac{1}{2}\pi[l_1+l_3+1-\frac{1}{2}(\tau_1+\tau_3)]\}}{\zeta_{l_1}\zeta_{l_3}}, \qquad (2.11)$$

$$\zeta_l = \begin{cases} \sin(\frac{1}{2}\pi l) & \text{if } \tau = +, \\ \cos(\frac{1}{2}\pi l) & \text{if } \tau = -. \end{cases}$$

which is derived in Gribov's original work, we obtain for the energy factors and ξ_{l_3} times the factor in brackets in (2.9)

$$s_{ab}{}^{l_1+l_3-1} s_{bc}{}^{l_2+l_3-1}\,(\eta^{-(l_1+l_3-1)}\xi_{l_1+l_3-1}\xi_{l_2 l_1} V_L i\gamma_{l_1 l_3} + \eta^{-(l_2+l_3-1)}\xi_{l_2+l_3-1}\xi_{l_1 l_2} V_R i\gamma_{l_2 l_3}). \qquad (2.12)$$

When we insert this into (2.9) and write it as a double Mellin transform like (2.6), then j_1 becomes equal to l_1+l_3-1 and $j_2 = l_2+l_3-1$. Since $\xi_{l_2 l_1}$ depends only on the difference l_2-l_1, which is now j_2-j_1, we obtain for the Mellin transform

$$\left(-\frac{1}{4i}\right)^2 \int dj_1 dj_2 s_{ab}{}^{j_1} s_{bc}{}^{j_2} \times(\eta^{-j_1}\xi_{j_1}\xi_{j_2 j_1} F_L + \eta^{-j_2}\xi_{j_2}\xi_{j_1 j_2} F_R), \qquad (2.13)$$

with

$$F_{\{L,R\}} = \int \frac{d^2k_\perp}{(2\pi)^2}\int \frac{dl_1 dl_2 dl_3}{(2\pi i)^3}\,\delta(l_1+l_3-1-j_1)\delta(l_2+l_3-1-j_2) \times N_{l_1 l_3} N_{l_2 l_3} G_{l_1}((q_1-k)_\perp{}^2) G_{l_2}((q_2-k)_\perp{}^2) G_{l_3}(k_\perp{}^2) V_{\{L,R\}} \gamma_{\{l_1,l_2\} l_3} \qquad (2.14)$$

and

$$\gamma_{\{l_1,l_2\} l_3} = \gamma_{l_1 l_3}$$

for F_L and

$$\gamma_{\{l_1,l_2\} l_3} = \gamma_{l_2 l_3}$$

for F_R. The reader realizes that (2.13) is indeed identical to (2.6) and only F_L and F_R have changed. Comparing (2.14) with the Reggeon diagram (Fig. 2 or Fig. 4) one further recognizes the field-theoretical structure which is very similar to the $2\to 2$ case: for each Reggeon line a propagator G, conservation of the two-dimensional momentum at each of the three vertices $N_{l_1 l_3}$, $N_{l_2 l_3}$, and V. Further, we have a loop integration $\int d^2k_\perp dl$. What is new, however, is the role of angular momentum. To the left-hand side of the produced particle, the sum of (angular momentum -1) is j_1-1 and on the right-hand side it is j_2-1, which are the exponents of s_{ab} and s_{bc}, respectively. In the language of field theory, the Reggeon "energy" j_1-1 enters the diagram from the left-hand side,

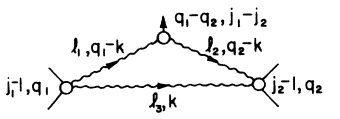

FIG. 4. Reggeon diagram as obtained from Fig. 2.

and the energy j_2-1 is leaving at the right-hand side. At the vertex of the produced particle we have a loss of energy $(j_2-1)-(j_1-1)=j_2-j_1$.

At this point we want to say a few words about the γ factors appearing in (2.14). In the analysis of the Mandelstam graph (Fig. 3), Gribov pointed out that $\gamma_{l_1 l_2}$ produces a zero when $j = l_1+l_2-1$ is a physical angular momentum. Consequently, the two-Reggeon cut contained in Fig. 3 does not contribute to physical partial waves in the t channel. In our case (2.14), the γ's play exactly the same role: F_L, being the coefficient of ξ_{j_1}, must vanish at physical values of j_1, because our diagram contains a two-Reggeon cut in j_1 and does not contribute to physical partial waves. This vanishing is ensured by $\gamma_{l_1 l_3}$. For F_R, the decoupling is provided by $\gamma_{l_2 l_3}$.

So far we have assumed that the blobs in Figs. 1 and 2 are simple Regge poles (therefore diagram Fig. 4). But from the way in which the asymptotic behavior of such hybrid Feynman diagrams is derived, it is clear that the blobs can also be more complicated subamplitudes which contain cuts, e.g., Fig. 5(a). If the blobs in Fig. 5 are poles, we obtain the Reggeon diagram Fig. 5(b). The asymptotic behavior of this diagram is again (2.13), but in (2.14) $N_{l_1 l_3}$ and $N_{l_2 l_3}$ have to be replaced by two-particle–three-Reggeon coupling functions and the Reggeon propagators G_{l_1} and G_{l_3} replaced by more complicated Green's functions [Fig. 5(c)], e.g.

$$N_{l_1 l_3} G_{l_1} \to \int \frac{d^2k'}{(2\pi)^2} \int \frac{dl_1' dl_1''}{(2\pi i)^2} N_{l_1' l_1'' l_3} \gamma_{l_1' l_1''} \delta(l_1' + l_1'' - l_1 - 1) G_{l_1'}(k_\perp'^2) G_{l_1''}((q_1 - k - k_1')_\perp^2) \gamma_{l_1' l_1''; l_1} G_{l_1} \,. \tag{2.15}$$

The rules for the calculation of these "self-energy" corrections are the same as in the analysis of $2 \to 2$ scattering.

Next we analyze diagrams of the form Fig. 6, where the left-hand side (lhs) may be any $2 \to 2$ amplitude which can be calculated by use of the familiar rules, and the right-hand side (rhs) may be any $2 \to 3$ amplitude which we have considered so far. For illustration, we take the simple diagram of Fig. 7(a) with Regge poles for the blobs, but our considerations will also be valid for more complicated amplitudes. In Fig. 7(a), the subamplitudes have the representations

$$F_{\text{lhs}} = -\frac{1}{4i} \int dl\, \xi_l [(p_1 - k)^2]^l \frac{g(t_1)^2}{l - \alpha(t_1)} \,, \tag{2.16}$$

$$F_{\text{rhs}} = \left(\frac{-1}{4i}\right)^2 \int dj_1 dj_2 [(k - q_2)^2]^{j_1} s_{bc}^{\,j_2} \times (\eta^{-j_1} \xi_{j_1 j_2 j_1} F_L + \eta^{-j_2} \xi_{j_2 j_1 j_2} F_R) \,, \tag{2.17}$$

with $F_{L,R}$ taken from (2.14). The study of the link between the two amplitudes follows the pattern of Gribov's analysis in the $2 \to 2$ case: One uses Sudakov variables: $k = \alpha p_2' + \beta p_1' + k_\perp$ [cf. (A1)]; and from the requirement that the external masses of F_{lhs} and F_{rhs} are to be finite when all energies are large we obtain

$$\left.\begin{aligned} k^2 &= s\alpha\beta + k_\perp^2 \sim m^2 \\ (q_1 - k)^2 &= -s_{bc}\alpha + s\alpha\beta + (q_1 - k)_\perp^2 \sim m^2 \end{aligned}\right\} \to |\alpha| \lesssim \frac{m^2}{s_{bc}} \,, \quad k_\perp^2 \lesssim m^2 \,, \tag{2.18}$$

$$\left.\begin{aligned} (p_1 - k)^2 &\sim -\alpha s \gg m^2 \\ (p_2 + k)^2 &\sim \beta s \gg m^2 \\ (k - q_2)^2 &\sim \beta s_{ab} \gg m^2 \end{aligned}\right\} \to |\alpha| \gg \frac{m^2}{s} \,, \quad |\beta| \gg \frac{m^2}{s_{ab}} \,. \tag{2.19}$$

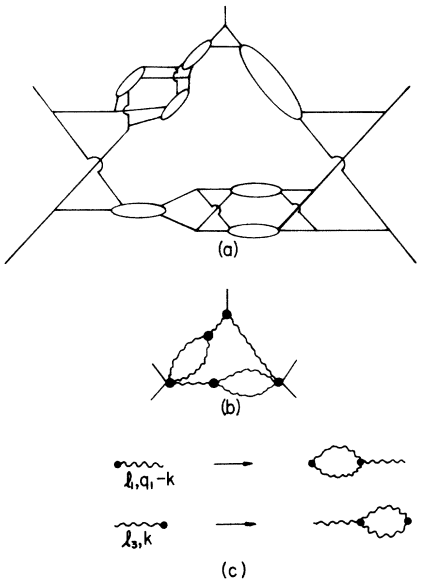

FIG. 5. This diagram is obtained from Fig. 2 when the blobs there have a more complicated internal structure. (a) Hybrid Feynman diagram; (b) Reggeon diagram to (a); (c) replacements to be made in Fig. 4 in order to reach Fig. 5(b).

Thus the α, β integrations are restricted to

$$\frac{m^2}{s} \ll |\alpha| \lesssim \frac{m^2}{s_{bc}} \,, \quad \frac{m^2}{s_{ab}} \ll |\beta| \lesssim 1 \,. \tag{2.20}$$

But when $\beta \sim 1$, (2.18) requires $s\alpha\beta \sim m^2$ and $\alpha \sim m^2/s$, whereas (2.19) demands $\alpha s \gg m^2$. Similarly, $\alpha \sim m^2/s_{bc}$ implies $\beta \sim m^2/s_{ab}$ and $(k - q_2)^2$ is no longer large. Therefore, (2.20) is replaced by

$$\frac{m^2}{s} \ll |\alpha| \ll \frac{m^2}{s_{bc}} \,, \quad \frac{m^2}{s_{ab}} \ll |\beta| \ll 1 \tag{2.21}$$

and, as a consequence of this, we are allowed to approximate $(q_1 - k)^2$ in (2.18):

$$(q_1 - k)^2 \sim s\alpha\beta + (q_1 - k)_\perp^2 \,. \tag{2.22}$$

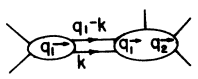

FIG. 6. Another diagram for the $2 \to 3$ amplitude.

So the link becomes

$$\int d^4k F_{\rm lhs}\,\frac{1}{k^2-m^2}\,\frac{1}{(q_1-k)^2-m^2}\,F_{\rm rhs}=\left(-\frac{1}{4i}\right)^2\int dl\,dj_1 s\int d\alpha\,d\beta(-\alpha s)^l\xi_l(\beta s_{ab})^{j_1}\times\frac{1}{s\alpha\beta+k_\perp^2-m^2}\,\frac{1}{s\alpha\beta+(k-q_1)_\perp^2-m^2}\cdots, \tag{2.23}$$

where we have written down only those terms which show the dependence on α and β. For the α integration there are poles from the two propagators (and the external masses of $F_{\rm rhs}$, $F_{\rm lhs}$) lying exclusively on one side of the real α axis, as well as from the energy cut of $F_{\rm lhs}$, one in the upper and one in the lower half plane. Since one half plane is always free from the propagator poles (for $\beta>0$ it is the upper, for $\beta<0$ it is the lower half plane), we can close the α integration contour around the energy cut in this half plane and obtain the integral of the energy discontinuity. Furthermore, the two contributions due to $\beta>0$ and $\beta<0$ just cancel each other if $F_{\rm lhs}$ is opposite to the s_{ab} signature in $F_{\rm rhs}$, but add if they are equal. Thus (2.23) becomes

$$2\left(-\frac{1}{4i}\right)^2\int dl\,dj_1 s\int_{-m^2/s}^{-m^2/s_{bc}}d\alpha\int_{m^2/s_{ab}}^{1}d\beta(-\alpha s)^l(\beta s_{ab})^{j_1}\int d^2k_\perp\,\frac{1}{s\alpha\beta+k_\perp^2-m^2}\,\frac{1}{s\alpha\beta+(k-q_1)_\perp^2-m^2}\,, \tag{2.24}$$

where the signature factor ξ_l has disappeared, because we have taken the energy discontinuity of $F_{\rm lhs}$. Since all terms in (2.24) to the right of the energy factors depend only on $s\alpha\beta$ but not α or β separately, we introduce $x=-s\alpha\beta$ as a new variable and perform the β integration:

$$s\int_{-m^2/s}^{-m^2/s_{bc}}d\alpha\int_{m^2/s_{ab}}^{1}d\beta(-\alpha s)^l(\beta s_{ab})^{j_1}=s_{ab}{}^{j_1}\int_{m^2/s_{ab}}^{1}d\beta\,\beta^{j_1-l-1}\int dx\,x^l\cdots. \tag{2.25}$$

The most singular part will come from $j_1\sim l$, where (2.25) becomes

$$\frac{s_{ab}{}^{j_1}-s_{ab}{}^{l}}{j_1-l}\int dx\,x^l\cdots. \tag{2.26}$$

Finally, we take the Mellin transform in s_{ab} of the whole expression and perform the l and j_1 integrations:

$$\left(-\frac{1}{4i}\right)^2\int dj\,dj_2 s_{ab}{}^{j}s_{bc}{}^{j_2}\Big[\eta^{-j}\xi_j\xi_{j_2 j}g(t_1)G_j(t_1)\left(2\int\frac{d^2k_\perp}{(2\pi)^2}\int dx\,x^j\,\frac{g(t_1)}{-x+k_\perp^2-m^2}\,\frac{1}{-x+(k-q)_\perp^2-m^2}\right)F_L$$
$$+\eta^{-j_2}\xi_{j_2 j}\xi_{jj_2}g(t_1)G_j(t_1)\left(2\int\frac{d^2k_\perp}{(2\pi)^2}\int dx\,x^j\,\frac{g(t_1)}{-x+k_\perp^2-m^2}\,\frac{1}{-x+(k-q)_\perp^2-m^2}\right)F_R\Big]. \tag{2.27}$$

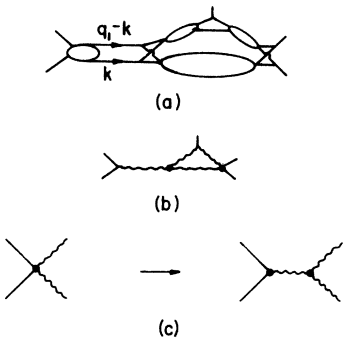

FIG. 7. This diagram can be obtained by "enhancing" the left crossed box graph in Fig. 2 through pole exchange. (a) Hybrid Feynman diagram; (b) corresponding Reggeon diagram; (c) replacement to be made in Fig. 4 in order to reach Fig. 7(b).

It differs from (2.13) in that F_L and F_R there are replaced by

$$F_{L,R}\to g(t_1)G_j(t_1)r_jF_{L,R}$$

[where r_j stands for the quantity in curved parentheses in (2.27)]. This corresponds to Fig. 7(c), and the rules for this replacement are the same as in the $2\to2$ case. Clearly, (2.27) is again of the form (2.6) with modified $F_{L,R}$.

Let us stop here for a moment and see what we learn from these considerations. What we have demonstrated is that internal Reggeon-Reggeon-Reggeon vertices in the $2\to3$ amplitude obey the same rules as in the $2\to2$ case. In particular, this means that momentum and Reggeon energies

(= angular momentum −1) are conserved. Combining this with what we have said following (2.14), we obtain the rules for a Reggeon field theory which is, apart from the new vertex V and the fact that we now have two different Reggeon energies $j_1 - 1$, $j_2 - 1$, the same as in the $2 \to 2$ case.

Before we are justified in stating this as our result for the $2 \to 3$ amplitude it is necessary to consider a somewhat larger class of Reggeon diagrams. To this end we look at the hybrid-Feynman diagrams of Fig. 8 and the corresponding Reggeon diagrams in Fig. 9. Their analysis is rather lengthy and described in the Appendix. Again the amplitudes are of the form (2.6), and $F_{L,R}$ are calculated with our field-theoretic rules stated above. Thus our result is completely confirmed, and we summarize our rules as follows:

(a) Write the $2 \to 3$ amplitude in the form (2.6). For the computation of $F_{L,R}(j_1 j_2 t_1 t_2 \eta)$ use the following rules.

(b) Each Reggeon line has the same direction (say, to the right) and carries energy $l - 1$ and momentum $\vec{k}_\perp$. It corresponds to the propagator $G_l(k_\perp^2) = 1/[l - \alpha(k_\perp^2)]$, and the l integration, whose contour runs to the right of the propagator pole, is to be closed to the left around the pole.

(c) Any internal n-Reggeon $\to m$-Reggeon vertex [Fig. 10(a)] is denoted by $\gamma_{l_1 \cdots l_n ; l_1' \cdots l_m'}$ and is accompanied by conservation of energy and momentum: $\sum_1^n \vec{k}_i = \sum_1^m \vec{k}_i'$ and $\sum_1^n (l_i - 1) = \sum_1^m (l_i' - 1)$.

(d) For the two-particle–n-Reggeon vertex [Fig. 10(b)] there is a factor $N_{l_1 \cdots l_n}$ and conservation of energy and momentum: At the left vertex $\vec{q}_1 = \sum \vec{k}_i$, $j_1 - 1 = \sum (l_i - 1)$, and at the right one $\vec{q}_2 = \sum \vec{k}_i$, $j_2 - 1 = \sum (l_i - 1)$.

(e) A factor $V_L(l_1, l_2; k_{1\perp}^2, k_{2\perp}^2, \eta)$ or $V_R(l_1, l_2; k_{1\perp}^2, k_{2\perp}^2, \eta)$ as well as a conservation $\vec{k}_1 - \vec{k}_2 = (\vec{q}_1 - \vec{q}_2)$, $l_1 - l_2 = (j_1 - j_2)$ for the one-particle–two-Reggeon vertex [Fig. 10(c)] exists.

(f) For each closed loop there is an integration $\int d^2k\, dl/(2\pi)^3 i$. Any diagram is then of the form

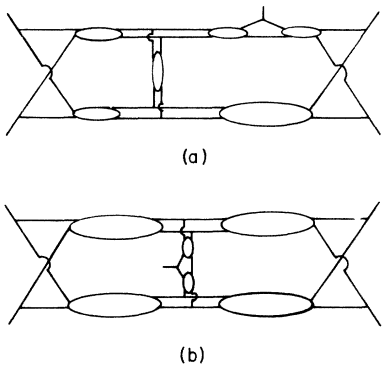

FIG. 8. Two more complicated diagrams.

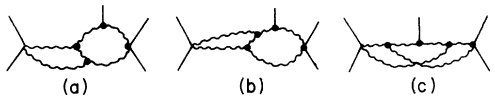

FIG. 9. Reggeon diagrams, obtained from Fig. 8.

of Fig. 11: $j_1 - 1$, $\vec{q}_1$ are total energy and momentum on the left side, $j_2 - 1$, $\vec{q}_2$ those on the right side of the produced particle, and $j_1 - j_2$, $\vec{q}_1 - \vec{q}_2$ is leaving along the produced particle.

(g) Finally, each vertex with $n > 1$ outgoing Reggeons is accompanied by a factor $\gamma_{l_1 \cdots l_n}$, which in analogy to (2.11) is defined by

$$\xi_{l_1} \cdots \xi_{l_n} = (i)^{n-1} \gamma_{l_1 \cdots l_n} \xi_{l_1 + \cdots + l_n - (n-1)} \,. \tag{2.28}$$

In addition to that, there is a factor $1 = \gamma_{l j_1 + 1 - l} / \gamma_{l j_1 + 1 - l}$ for the l loop in F_L and $\gamma_{l j_2 + 1 - l} / \gamma_{l j_1 + 1 - l}$ in F_R. (See Fig. 11 for the definition of the l loop.)

This last rule needs a comment. By combining γ factors in the diagram in an appropriate way and by using identities like

$$\gamma_{l_1 l_2 + l_3 - 1} \gamma_{l_2 l_3} = \gamma_{l_2 l_1 + l_3 - 1} \gamma_{l_1 l_3} \tag{2.29}$$

one can always cancel the $1/\gamma_{l j_1 + 1 - l}$. So there is no pole due to a zero at integer j_1. The numerators $\gamma_{l j_1 + 1 - l}$ and $\gamma_{l j_2 + 1 - l}$, however, are necessary if the diagram is to decouple from the physical angular momentum states of j_1, j_2, respectively. On the other hand, in practical calculations the vertices are approximated by constants and the γ's by their value at $l_i = 1$. Then the ratio in (g) reduces to 1 and we have just a $\sqrt{-1} = i$ for each vertex $\gamma_{l_1 ; l_2, l_3}$ and $N_{l_1 l_2}$ of the diagram, but not for the vertex of the produced particle.

The next step in enlarging the class of considered diagrams includes those of Figs. 12 and 13. They contain a new vertex which has not been studied as yet: the particle–three-Reggeon vertex. A detailed analysis of this vertex within the framework of Gribov's Sudakov technique, together with a brief study of diagrams that contain this vertex, will be given elsewhere.[8] Here we only mention that there are two different types. An example of the first type is given in Fig. 14(a). The resulting amplitude has again the form (2.6),

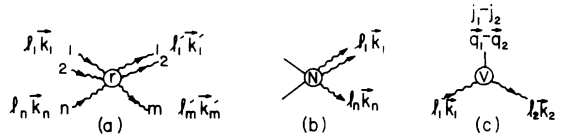

FIG. 10. Three types of vertices which occur in the Reggeon calculus for the production amplitude.

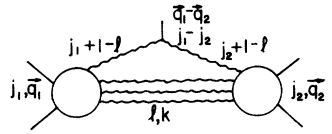

FIG. 11. Typical form of a Reggeon diagram in the $2\to 3$ amplitude.

i.e., two terms each of which corresponds to a set of simultaneous discontinuities (Fig. 4 of paper I). The other type [Fig. 14(b)], however, contributes only to one of these sets. In other words, Fig. 14(b) has no simultaneous singularities in s and s_{ab} and leads to the amplitude

$$T_{2\to 3}=\left(-\frac{1}{4i}\right)^2\int dj_1 dj_2 s_{ab}^{\,j_1}s_{bc}^{\,j_2}\eta^{-j_1}\xi_{j_1}\xi_{j_2 j_1}F_L(j_1 j_2 t_1 t_2\eta)\,, \tag{2.30}$$

$$F_L=g(t_1)G_{j_1}(t_1)\int\frac{d^2k}{(2\pi)^2}\int\frac{dl_1 dl_2}{(2\pi i)^2}\,\delta(l_1+l_2-1-j_2)W_L G_{l_1}(q_2-k)_\perp{}^2 G_{l_2}(k_\perp{}^2)N_{l_1 l_2}\,, \tag{2.31}$$

where W_L stands for the crossed box graph at the produced particle. Note that there is no contribution to F_R from this diagram. The fact that there exist these two types of a particle–three-Reggeon vertex is in agreement with what is expected from the partial-wave analysis in the crossed channel.[9] Apart from this the particle–three-Reggeon vertex fits into our Reggeon diagram technique: Amplitudes containing such a vertex are still of the form (2.6), and in the Reggeon field theory we have a new vertex where momentum is conserved and the produced particle carries away the Reggeon energy j_1-j_2, which is the difference of the Reggeon energy on the left-hand side and the total Reggeon energy on the right-hand side of the produced particle (Fig. 15). For particle–four-Reggeon and higher vertices we expect a generalization of these features: There will be several types of vertex functions and some of them will contribute only to one set of simultaneous singularities. However, we strongly expect that they will fit into our rules.

III. THE $2\to 4$ AMPLITUDE

In this section we shall consider some diagrams for the $2\to 4$ amplitude. From the results it will then be clear how to generalize the Reggeon diagram technique to the general $2\to n$ case. First we say a few words about the variables (Fig. 16).

The momentum-transfer vectors are

$$q_1=\frac{s_{bcd}-m^2}{2s}(p_1+p_2)+\frac{s_{bcd}-m^2-2q_1{}^2}{2(s-4m^2)}(p_1-p_2)+q_{1\perp}\,, \tag{3.1}$$

$$q_2=\frac{s_{cd}-s_{ab}}{2s}(p_1+p_2)+\frac{s_{cd}+s_{ab}-2m^2-2q_2{}^2}{2(s-4m^2)}(p_1-p_2)+q_{2\perp}\,, \tag{3.2}$$

$$q_3=\frac{m^2-s_{abc}}{2s}(p_1+p_2)+\frac{s_{abc}-m^2-2q_3{}^2}{2(s-4m^2)}(p_1-p_2)+q_{3\perp}\,. \tag{3.3}$$

The multi-Regge limit for this process is defined as

$$s, s_{abc}, s_{bcd}, s_{ab}, s_{bc}, s_{cd}\to\infty$$

$$\frac{s_{abc}}{s},\ \frac{s_{bcd}}{s},\ \frac{s_{ab}}{s_{abc}},\ \frac{s_{bc}}{s_{abc}},\ \frac{s_{bc}}{s_{bcd}},\ \frac{s_{cd}}{s_{bcd}}\to 0 \tag{3.4}$$

$$t_1=q_1{}^2,\ t_2=q_2{}^2,\ t_3=q_3{}^2 \text{ fixed.}$$

For each produced particle we have an η variable:

$$\eta_b=\frac{s_{ab}s_{bc}}{s_{abc}},\quad \eta_c=\frac{s_{bc}s_{cd}}{s_{bcd}}\,, \tag{3.5}$$

which in the multi-Regge limit become

$$\eta_b=m^2-(q_1-q_2)_\perp{}^2,\quad \eta_c=m^2-(q_2-q_3)_\perp{}^2\,. \tag{3.6}$$

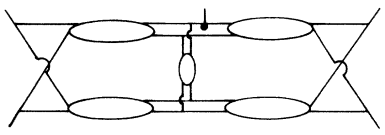

FIG. 12. A diagram which contains a three-Reggeon–particle vertex.

FIG. 13. Reggeon diagrams, obtained from Fig. 12.

There we have also the identities

$$\frac{s_{abc}s_{bcd}}{s} = s_{bc} ,$$

$$\frac{s_{abc}s_{cd}}{s} = \eta_c , \quad \frac{s_{ab}s_{bcd}}{s} = \eta_b . \tag{3.7}$$

$$t_1 = q_{1\perp}^2, \quad t_2 = q_{2\perp}^2, \quad t_3 = q_{3\perp}^2 .$$

As the simplest diagram for this process we consider Fig. 16(a), which reduces to Fig. 16(b) when the blobs are Regge poles. Its asymptotic behavior is (3.4) of paper I with V_L, V_R being the same functions as in the $2 \to 3$ amplitude of Fig. 1 [(2.5)]. For our following discussions we prefer to use a slightly different form. Using the η variables (3.5) and (3.7), we express all energies in terms of s_{ab}, s_{bc}, s_{cd}, η_b, and η_c. Then (3.4) of paper I becomes

$$\begin{aligned} T_{2\to 4} = s_{ab}{}^{\alpha_1} s_{bc}{}^{\alpha_2} s_{cd}{}^{\alpha_3} g(t_1)g(t_3)[&\xi_{\alpha_1}\xi_{\alpha_2\alpha_1}\xi_{\alpha_3\alpha_2}\eta_b{}^{-\alpha_1}\eta_c{}^{-\alpha_2}V_L(\eta_b)V_L(\eta_c) + \xi_{\alpha_2}\xi_{\alpha_1\alpha_2}\xi_{\alpha_3\alpha_2}\eta_b{}^{-\alpha_2}\eta_c{}^{-\alpha_2}V_R(\eta_b)V_L(\eta_c) \\ &+ \xi_{\alpha_3}\xi_{\alpha_2\alpha_3}\xi_{\alpha_1\alpha_2}\eta_b{}^{-\alpha_2}\eta_c{}^{-\alpha_3}V_R(\eta_b)V_R(\eta_c) \\ &+ (\xi_{\alpha_1}\xi_{\alpha_3\alpha_1}\xi_{\alpha_2\alpha_3} + \xi_{\alpha_3}\xi_{\alpha_1\alpha_3}\xi_{\alpha_2\alpha_1})\eta_b{}^{-\alpha_1}\eta_c{}^{-\alpha_3}V_L(\eta_b)V_R(\eta_c)] . \end{aligned} \tag{3.8}$$

It can also be written as a triple Mellin transform,

$$\left(-\frac{1}{4i}\right)^3 \int dj_1 dj_2 dj_3 s_{ab}{}^{j_1} s_{bc}{}^{j_2} s_{cd}{}^{j_3} \xi_{j_1}\xi_{j_2 j_1}\xi_{j_3 j_2}\eta_b{}^{-j_1}\eta_c{}^{-j_2}F_{LL} + \cdots , \tag{3.9}$$

$$F_{LL}(j_1 j_2 j_3 t_1 t_2 t_3 \eta_b \eta_c) = \left(\frac{2}{\pi}\right)^3 g(t_1)G_{j_1}(t_1)V_L(\eta_b)G_{j_2}(t_2)V_L(\eta_c)G_{j_3}(t_3)g(t_3) , \tag{3.10}$$

with a similar representation for the other four terms in (3.8) with functions F_{RL}, F_{RR}, F_{LR} analogous to (3.10). We shall now demonstrate that this form remains valid when cuts are included and that the rules for the cut contributions to the F's are a direct generalization of the $2 \to 3$ case.

To this end we first consider the diagram of Fig. 17. Its asymptotic behavior has been analyzed in Ref. 6 and we use the result[10]

$$\begin{aligned} i\left(\frac{\pi}{2}\right) \int \frac{dl_1 \cdots dl_4}{(2\pi i)^4} \frac{d^2k_\perp}{(2\pi)^2} N_{l_1 l_4} N_{l_3 l_4} G_{l_4}(k_\perp^2) G_{l_1}((q_1 - k)_\perp^2) G_{l_2}((q_2 - k)_\perp^2) G_{l_3}((q_3 - k)_\perp^2) s_{ab}{}^{l_1} s_{bc}{}^{l_2} s_{cd}{}^{l_3} s^{l_4 - 1} \\ \times \xi_{l_4}[\xi_{l_1}\xi_{l_2 l_1}\xi_{l_3 l_2}\eta_b{}^{-l_1}\eta_c{}^{-l_2}V_L(\eta_b)V_L(\eta_c) + \cdots] , \end{aligned} \tag{3.11}$$

where we did not write down the other four terms of (3.8). We reexpress s through $s_{ab}, s_{bc}, s_{cd}, \eta_b, \eta_c$ [(3.5), (3.7)],

$$s = \frac{s_{ab}s_{bc}s_{cd}}{\eta_b \eta_c} , \tag{3.12}$$

and write the energy factors in (3.11):

$$s_{ab}{}^{l_1 + l_4 - 1} s_{bc}{}^{l_2 + l_4 - 1} s_{cd}{}^{l_3 + l_4 - 1} \eta_b{}^{-(l_4 - 1)} \eta_c{}^{-(l_4 - 1)} . \tag{3.13}$$

Next we combine the signature factor ξ_{l_4} with ξ_{l_1}, using (2.11),

$$\xi_{l_1}\xi_{l_4} = i\gamma_{l_1 l_4}\xi_{l_1 + l_4 - 1} .$$

For the other four terms, we put together ξ_{l_4} with ξ_{l_2}, ξ_{l_3}, ξ_{l_1}, and ξ_{l_3}, respectively. In this way, we ob-

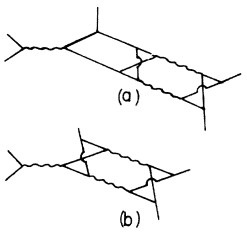

FIG. 14. The simplest diagrams with a three-Reggeon–particle vertex.

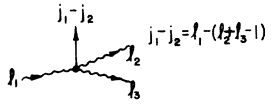

FIG. 15. The three-Reggeon–particle vertex.

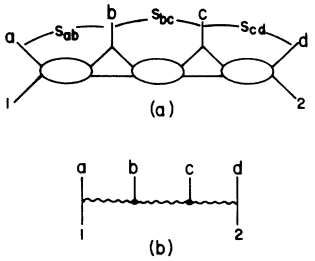

FIG. 16. The simplest diagram for the $2 \to 4$ amplitude.

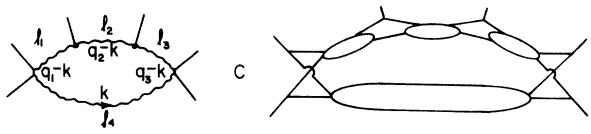

FIG. 17. A Regge cut in the $2 \to 4$ amplitude.

tain for energy factors, signature, and the first term in brackets in (3.11)

$$s_{ab}{}^{l_1+l_4-1}s_{bc}{}^{l_2+l_4-1}s_{cd}{}^{l_3+l_4-1}\xi_{l_1+l_4-1}\xi_{l_2l_1}\xi_{l_3l_2}\eta_b{}^{-(l_1+l_4-1)}\eta_c{}^{-(l_2+l_4-1)}i\gamma_{l_1l_4}V_LV_L\,. \tag{3.14}$$

Finally, we write (3.11) as a triple Mellin transformation:

$$T_{2\to4}=\left(-\frac{1}{4i}\right)^3\int dj_1dj_2dj_3s_{ab}{}^{j_1}s_{bc}{}^{j_2}s_{cd}{}^{j_3}(\xi_{j_1}\xi_{j_2j_1}\xi_{j_3j_2}\eta_b{}^{-j_1}\eta_c{}^{-j_2}F_{LL}+\cdots)\,, \tag{3.15}$$

with

$$F_{LL}=\int\frac{dl_1\cdots dl_4}{(2\pi i)^4}\int\frac{d^2k_\perp}{(2\pi)^2}(2\pi i)^3\delta(l_1+l_4-1-j_1)\delta(l_2+l_4-1-j_2)\delta(l_3+l_4-1-j_3)$$
$$\times G_{l_1}((q_1-k)_\perp{}^2)G_{l_2}((q_2-k)_\perp{}^2)G_{l_3}((q_3-k)_\perp{}^2)G_{l_4}(k_\perp{}^2)N_{l_1l_4}N_{l_3l_4}\gamma_{l_1l_4}V_L(\eta_b)V_L(\eta_c)\,. \tag{3.16}$$

Quite analogous expressions hold for the other four terms in (3.15). Again note the factors $\gamma_{l_1l_4}$ which decouple our diagram from the physical partial wave in the j_1 channel.

This consideration already indicates how to generalize the rules from the $2 \to 3$ amplitude to the $2 \to 4$ case. We now have three angular momenta j_1, j_2, and j_3, and j_1-1, j_2-1, j_3-1 are just the sums of the energies of the Reggeons cut by cutting the diagram in Fig. 17 vertically to the left of particle b, between b and c, and to the right of particle c, respectively. Equivalently, the Reggeon energy j_1-1 enters the diagram from the left-hand side, j_3-1 leaves on the right end, and particles b and c carry away j_1-j_2, j_2-j_3, respectively. With this prescription, we again have our familiar Reggeon field theory.

We want to demonstrate the validity of these rules still in a few other Reggeon diagrams. Taking that of Fig. 18 we again quote the result of Ref. 6 where the diagram has been analyzed[11]:

$$i\left(\frac{\pi}{2}\right)^3\int\frac{dl_1\cdots dl_4}{(2\pi)^4}\int\frac{d^2k_\perp}{(2\pi)^2}N_{l_1l_3}N_{l_2l_4}G_{l_1}(k_\perp{}^2)G_{l_2}((q_3-q_2-k)_\perp{}^2)G_{l_3}((q_1+k)_\perp{}^2)G_{l_4}((q_2+k)_\perp{}^2)s_{ab}{}^{l_3}s_{bcd}{}^{l_4}s_{abc}{}^{l_1}s_{cd}{}^{l_2}$$
$$\times[\eta_c{}^{-l_1}V_L(\eta_c)\xi_{l_1\xi_{l_2l_1}}+\eta_c{}^{-l_2}V_R(\eta_c)\xi_{l_2}\xi_{l_1l_2}][\eta_b{}^{-l_3}V_L(\eta_b)\xi_{l_3}\xi_{l_4l_3}+\eta_b{}^{-l_4}V_R(\eta_b)\xi_{l_4}\xi_{l_3l_4}]\,. \tag{3.17}$$

The energy factors are transformed into

$$s_{ab}{}^{l_1+l_3-1}s_{bc}{}^{l_1+l_4-1}s_{cd}{}^{l_2+l_4-1}\eta_c{}^{-(l_4-1)}\eta_b{}^{-(l_1-1)} \tag{3.18}$$

and for the phase factors we combine

$$\begin{aligned}
&\xi_{l_1}\xi_{l_3}\xi_{l_2l_1}\xi_{l_4l_3}=i\gamma_{l_1l_3}\xi_{l_1+l_3-1}\xi_{l_2l_1}\xi_{l_4l_3}\,,\\
&\xi_{l_1}\xi_{l_4}\xi_{l_2l_1}\xi_{l_3l_4}=i\gamma_{l_1l_4}\xi_{l_1+l_4-1}\xi_{l_2l_1}\xi_{l_3l_4}\,,\\
&\xi_{l_2}\xi_{l_4}\xi_{l_1l_2}\xi_{l_3l_4}=i\gamma_{l_2l_4}\xi_{l_2+l_4-1}\xi_{l_1l_2}\xi_{l_3l_4}\,.
\end{aligned} \tag{3.19}$$

For the combination of the remaining pair we need another identity,

$$\xi_{l_3}\xi_{l_4l_3}\xi_{l_2}\xi_{l_1l_2}=i\,\frac{\cos\{\frac{1}{2}\pi[l_1+l_3+1-\frac{1}{2}(\tau_1+\tau_3)]\}\sin\{\frac{1}{2}\pi[j_2-j_3+1-\frac{1}{2}(\tau_1-\tau_2)]\}}{\zeta_{l_2}\zeta_{l_3}}\xi_{j_1}\xi_{j_2j_3}\xi_{j_3j_1}$$
$$+i\,\frac{\cos\{\frac{1}{2}\pi[l_2+l_4+1-\frac{1}{2}(\tau_2+\tau_4)]\}\sin\{\frac{1}{2}\pi[j_2-j_1+1-\frac{1}{2}(\tau_4-\tau_3)]\}}{\zeta_{l_2}\zeta_{l_3}}\xi_{j_3}\xi_{j_2j_1}\xi_{j_1j_3}\,, \tag{3.20}$$

which can be checked by simple algebra. Here we have set $j_1 = l_1 + l_3 - 1$, $j_2 = l_1 + l_4 - 1$, $j_3 = l_2 + l_4 - 1$. Finally, we take the Mellin transform of (3.17),

$$T_{2\to4} = \left(-\frac{1}{4i}\right)^2 \int dj_1 dj_2 dj_3 s_{ab}{}^{j_1} s_{bc}{}^{j_2} s_{cd}{}^{j_3} [\eta_b{}^{-j_1}\eta_c{}^{-j_2} F_{LL} \xi_{j_1}\xi_{j_2 j_1}\xi_{j_3 j_2} + \eta_b{}^{-j_2}\eta_c{}^{-j_2} F_{RL}\xi_{j_2}\xi_{j_1 j_2}\xi_{j_3 j_2} + \eta_b{}^{-j_2}\eta_c{}^{-j_3} F_{RR}\xi_{j_3}\xi_{j_2 j_3}\xi_{j_1 j_2} + \eta_b{}^{-j_1}\eta_c{}^{-j_3} F_{LR}(\xi_{j_1}\xi_{j_3 j_1}\xi_{j_2 j_3} + \xi_{j_3}\xi_{j_1 j_3}\xi_{j_2 j_1})] \ , \tag{3.21}$$

which is again of the form (3.8). In the relation (3.20) one recognizes on the right-hand side the factors $\cos\{\frac{1}{2}\pi[l_1 + l_3 + 1 - \frac{1}{2}(\tau_1 + \tau_3)]\}$ and $\cos\{\frac{1}{2}\pi[l_2 + l_4 + 1 - \frac{1}{2}(\tau_1 + \tau_4)]\}$: They guarantee [cf. (2.11)] the decoupling of our diagram from the partial-wave amplitude at integers j_1 and j_3, respectively.

Our last example is the diagram in Fig. 19. For the subamplitudes on the right- and left-hand sides we use (2.13):

$$F_{\rm lhs} = \left(-\frac{1}{4i}\right)^2 \int dj_1 dl_2 s_{ab}{}^{j_1} [(q_1 - k)^2]^{l_2} [\xi_{j_1}\xi_{l_2 j_1} F_L(\eta_b)\eta_b{}^{-j_1} + \eta_b{}^{-l_2} F_R(\eta_b)\xi_{l_2}\xi_{j_1 l_2}] \ ,$$
$$F_{\rm rhs} = \left(-\frac{1}{4i}\right)^2 \int dl_3 dj_3 [(q_2 - k)^2]^{l_3} s_{cd}{}^{j_1} [\xi_{l_3}\xi_{j_3 l_3}\eta_c{}^{-l_3} F_L(\eta_c) + \xi_{j_3}\xi_{l_3 j_3}\eta_c{}^{-j_3} F_R(\eta_c)] \ . \tag{3.22}$$

The link between $F_{\rm lhs}$ and $F_{\rm rhs}$ is analyzed in the same way as used in Sec. II for Fig. 7:

$$\frac{m^2}{s_{bcd}} \ll |\alpha| \ll \frac{m^2}{s_{cd}} , \quad \frac{m^2}{s_{abc}} \ll |\beta| \ll \frac{m^2}{s_{ab}} \ , \tag{3.23}$$

$$T_{2\to4} = \frac{-i}{2(2\pi)^2} \int dl_2 dl_3 s \int d\alpha (-\alpha s_{bcd})^{l_2} \int d\beta (\beta s_{abc})^{l_3} \int \frac{d^2k_\perp}{(2\pi)^2} \frac{1}{s\alpha\beta + k_\perp{}^2 - m^2} \frac{1}{s\alpha\beta + (k - q_2)_\perp{}^2 - m^2}$$
$$\times \int dj_2 dj_3 s_{ab}{}^{j_1} s_{cd}{}^{j_3} [\xi_{j_1}\xi_{l_2 j_1}\xi_{l_3}\xi_{j_2 l_3}\eta_b{}^{-j_1}\eta_c{}^{-l_3} F_L(\eta_b) F_L(\eta_c) + \xi_{l_2}\xi_{j_1 l_2}\xi_{l_3}\xi_{j_3 l_3}\eta_b{}^{-l_2}\eta_c{}^{-l_3} F_R(\eta_b) F_L(\eta_c) + \xi_{l_2}\xi_{j_1 l_2}\xi_{j_3}\xi_{l_3 j_3}\eta_b{}^{-l_2}\eta_c{}^{-j_3} F_R(\eta_b) F_R(\eta_c) + \xi_{j_1}\xi_{l_2 j_1}\xi_{j_3}\xi_{l_3 j_3}\eta_b{}^{-j_1}\eta_c{}^{-j_3} F_L(\eta_b) F_R(\eta_c)] \ . \tag{3.24}$$

As to the α and β integrations, we close the contour of one of them around the energy cuts which are due to $(-\alpha s_{bcd})^{l_2}$ and $(\beta s_{abc})^{l_3}$ and obtain an integral of the discontinuity across the cut. To illustrate this for the first term in (3.24), we write the η's, energy, and signature factor as

$$(-s\alpha)^{j_1}(-\alpha s_{bcd})^{l_2 - j_1}\xi_{j_1}\xi_{l_2 j_1}(\beta s)^{l_3}(s_{cd})^{j_3 - l_3}\xi_{l_3}\xi_{j_3 l_3} \tag{3.25}$$

and see that β appears only in the total energy of $F_{\rm rhs}$ (Fig. 20). The discontinuity across its cut is just

$$\text{disc}_{\beta s}[(\beta s)^{l_3}(s_{cd})^{j_3 - l_3}\xi_{l_3}\xi_{j_3 l_3}] = -(\beta s)^{l_3} s_{cd}{}^{j_3 - l_3}\xi_{j_3 l_3} \ , \tag{3.26}$$

and by the same arguments as in the previous section we arrive at

$$2\int dl_2 dl_3 s \int_{-m^2/s_{bcd}}^{-m^2/s_{cd}} d\alpha (-\alpha s_{bcd})^{l_2} \int_{-m^2/s_{abc}}^{+m^2/s_{ab}} d\beta (\beta s_{abc})^{l_3} \int dj_1 dj_3 s_{ab}{}^{j_1} s_{cd}{}^{j_3}\xi_{j_1}\xi_{l_2 j_1}\xi_{j_3 l_3}$$
$$\times \int \frac{d^2k_\perp}{(2\pi)^2} \frac{1}{s\alpha\beta + k_\perp{}^2 - m^2} \frac{1}{s\alpha\beta + (k - q_2)_\perp{}^2 - m^2}$$
$$\times \eta_b{}^{-j_1}\eta_c{}^{-l_3} F_L(\eta_b) F_L(\eta_c) \ . \tag{3.27}$$

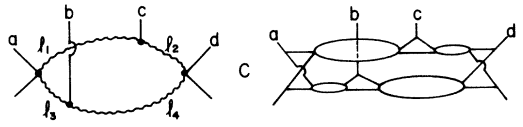

FIG. 18. Another diagram of the 2→4 amplitude.

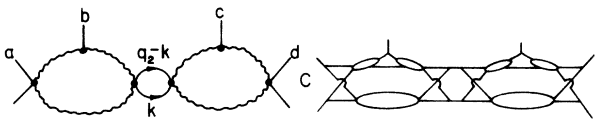

FIG. 19. Another diagram of the 2→4 amplitude.

Changing α and β to $\alpha' = \eta_c^{-1} s_{cd}\alpha$, $\beta' = \eta_b^{-1} s_{ab}\beta$ leads to

$$2\int dl_2 dl_3 s_{bc} \int_{-m^2/s_{bc}}^{-m^2/\eta_c} d\alpha' (-\alpha' s_{bc})^{l_2} \int_{m^2/s_{bc}}^{m^2/\eta_b} d\beta' (\beta' s_{bc})^{l_3} \int \frac{d^2k_\perp}{(2\pi)^2} \frac{1}{s_{bc}\alpha'\beta' + k_\perp^2 - m^2} \frac{1}{s_{bc}\alpha'\beta' + (k-q_s)_\perp^2} \cdots , \tag{3.28}$$

and introducing $x = -s_{bc}\alpha'\beta'$ and performing the β' integration gives

$$(3.28) = 2\int dl_2 dl_3 \frac{s_{bc}^{l_3}(m^2/\eta_b)^{l_3-l_2} - s_{bc}^{l_2}(m^2)^{l_3-l_2}}{l_3 - l_2} \int dx\, x^{l} \cdots . \tag{3.29}$$

Finally, we take the Mellin transform with respect to s_{bc} and perform the l_3, l_2 integrations by closing their contours to the right-hand side. The pole $1/(l_3 - l_2)$ makes $(m^2/\eta_b)^{l_3-l_2}$ and $(m^2)^{l_3-l_2}$ in (3.29) vanish, and we end up with

$$\left(-\frac{1}{4i}\right)^3 \int dj_1 dj_2 dj_3 s_{ab}^{j_1} s_{bc}^{j_2} s_{cd}^{j_3} \xi_{j_1 j_2 j_1} \xi_{j_2 j_3 j_2} \eta_b^{-j_1} \eta_c^{-j_2} \int \frac{d^2k_\perp}{(2\pi)^2} \int dx\, x^{j_2} F_L(\eta_b) \times \frac{1}{-x + k_\perp^2 - m^2} \frac{1}{-x + (k-q_2)_\perp^2 - m^2} F_L(\eta_c) . \tag{3.30}$$

A similar argument holds for the second and third terms in (3.24), but for the fourth we have

$$(-s\alpha)^{j_1}(-\alpha s_{bcd})^{l_2 - j_1} \xi_{j_1 l_2} (\beta s)^{j_3} (\beta s_{abc})^{j_3 - l_3} \xi_{l_3 j_3 l_3} . \tag{3.31}$$

Now β appears in both the total energy of $F_{\rm rhs}$ and the subenergy, and when we move the β contour around, we pick up the discontinuity across both energy cuts (Fig. 21):

$$F_{\rm rhs}(\beta s + i\epsilon, \beta s_{abc} + i\epsilon) - F_{\rm rhs}(\beta s - i\epsilon, \beta s_{abc} - i\epsilon) = \mathrm{disc}_{\beta s} F_{\rm rhs}(\beta s, \beta s_{abc} + i\epsilon) + \mathrm{disc}_{\beta s_{abc}} F_{\rm rhs}(\beta s - i\epsilon, \beta s_{abc}) = \left(-\frac{1}{4i}\right)^2 \int d\beta_3 dj_3 (\beta s)^{j_3} (\beta s_{abc})^{j_3 - l_3} (\xi_{j_3 l_3} + \xi_{l_3}^*) F_R(\eta_c) . \tag{3.32}$$

With this we reach the form (3.27) and, by repeating the steps, finally arrive at the analog of (3.30). For the combination of our signature factors we use the identity

$$(\xi_{j_3 j_2} + \xi_{j_2}^*)\xi_{j_1 j_2 j_1} = \xi_{j_1 j_3 j_1}\xi_{j_2 j_3 j_2} + \xi_{j_3}\xi_{j_2 j_3 j_2}\xi_{j_2 j_1} , \tag{3.33}$$

and have

$$\left(-\frac{1}{4i}\right)^3 \int dj_1 dj_2 dj_3 s_{ab}^{j_1} s_{bc}^{j_2} s_{cd}^{j_3} (\xi_{j_1 j_3 j_1}\xi_{j_2 j_3 j_2} + \xi_{j_3}\xi_{j_1 j_3 j_2 j_1}) \eta_b^{-j_1} \eta_c^{-j_3} \times \int \frac{d^2k_\perp}{(2\pi)^2} \int dx\, x^{j_2} F_L(\eta_b) \frac{1}{-x + k_\perp^2 - m^2} \frac{1}{-x + (k-q_2)_\perp^2 - m^2} F_R(\eta_c) . \tag{3.34}$$

This concludes our demonstration of the validity of our rules in more complicated diagrams.

IV. SUMMARY AND DISCUSSION

In the previous sections we examined hybrid Feynman diagrams which contain Regge-cut contributions to the $2 \to 3$ and $2 \to 4$ production amplitudes. In performing this analysis, we followed the pattern of Gribov's work on the $2 \to 2$ amplitude, and the result of our study is that Gribov's Reggeon calculus can be extended to the production amplitude. We found mainly three new features which are not present in the $2 \to 2$ case. The first one is the decomposition of the amplitude in-

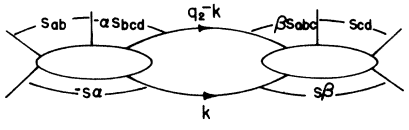

FIG. 20. A hybrid Feynman diagram which contains the diagrams of Fig. 19.

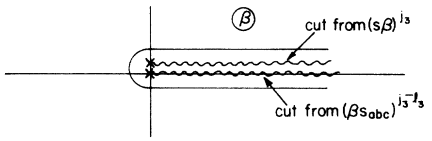

FIG. 21. Singularities of β of (3.31).

to a sum of terms, each of which reflects a certain singularity structure. In paper I we derived and discussed this representation for amplitudes which contain only Regge poles, but the calculations of the last two sections demonstrate that it remains valid when Regge cuts are included. If we take, for instance, the $2\to3$ process, then for any given Reggeon diagram the amplitude can be written in the form (1.2), and our rules then tell us how to compute F_L and F_R.

The second new phenomenon is the existence of more than one momentum variable and angular momentum, which in the Reggeon calculus plays the role of energy. In terms of Reggeon field theory, the $2\to2$ amplitude is a two-point function and depends only on one momentum and energy variable. In contrast to this, the functions $F_{L,R}$ of the $2\to3$ amplitude are three-point functions and depend on two Reggeon energies and momenta.

Finally, the diagrams for the $2\to n$ production process contain a new vertex which couples the produced particle to Reggeons. In the simplest case, it is a two-Reggeon–particle coupling, the analytic properties of which have been discussed by several authors, but, in general, the produced particle can also couple to three or more Reggeons. In this paper, we have been concerned only with the two-Reggeon–particle coupling, but our rules will include the more general coupling function. A discussion of diagrams with a three-Reggeon–particle vertex which will be given elsewhere[8] shows that this higher-order coupling indeed fits into our rules, and leads to the result that the same is true for the general many-Reggeon–particle coupling.

All these results have been derived from a study of $2\to3$ and $2\to4$ Reggeon diagrams. We expect, however, that our rules apply to the $2\to n$ amplitude. In fact, we have considered at least some types of $2\to n$ Reggeon graphs and found that our rules are correct. We do not want to present these calculations here, but we consider them as a justification for the expectation that our rules are of general validity.

After these remarks we want to list our rules. They are a direct extension of the rules for the $2\to3$ amplitude given at the end of Sec. III, and summarize the results of Sec. II and III. For the calculation of any Reggeon diagram that contributes to the $2\to n$ production amplitude, one proceeds in the following way:

(a) Write the $2\to n$ amplitude in the representation which we have described in paper I and write each term as a multiple Sommerfeld-Watson transform.

For illustration, a typical term of the $2\to5$ amplitude is [cf. (3.16) of paper I]

$$\left(-\frac{1}{4i}\right)^4\int dj_1\cdots dj_4 s^{j_3}S_{abc}{}^{j_1-j_3}S_{de}{}^{j_4-j_3}S_{bc}{}^{j_2-j_1}\xi_{j_3}\xi_{j_1j_3}\xi_{j_2j_1}\xi_{j_4j_3}F_{LRL}(t_1\cdots t_4,j_1\cdots j_4;\eta_b,\eta_c,\eta_d)$$

$$=\left(\frac{-1}{4i}\right)^4\int dj_1\cdots dj_4 s_{ab}{}^{j_1}S_{bc}{}^{j_2}S_{cd}{}^{j_3}S_{de}{}^{j_4}\xi_{j_3}\xi_{j_1j_3}\xi_{j_2j_1}\xi_{j_4j_3}\eta_b{}^{-j_1}\eta_c{}^{-j_3}\eta_d{}^{-j_3}F_{LRL}(\eta_b,\eta_c,\eta_d)\ . \quad (4.1)$$

The $n-2$ subscripts of F correspond to the set of $V_{R,L}$ functions to which it would reduce for pure pole exchange [cf. (3.16) of paper I], and reflect the singularity structure of this term.

For the calculation of the F functions, use the Reggeon diagram technique as follows:

(b) Each Reggeon line has the same direction, say to the right of the diagram, and carries energy $l-1$ and momentum $\vec{k}_\perp$. It corresponds to the propagator $G_l(k_\perp{}^2)=1/[l-\alpha(k_\perp{}^2)]$, and the l integration, whose contour lies to the right of the propagator pole, is to be closed to the left around the pole.

(c) Any internal n-Reggeon$\to m$-Reggeon vertex [Fig. 10(a)] has a factor $r_{l_1\cdots l_n;l_1'\cdots l_m'}$ and is associated with conservation of momentum and energy: $\sum_1^n\vec{k}_i=\sum_1^m\vec{k}_i'$, $\sum_1^n(l_i-1)=\sum_1^m(l_i'-1)$.

(d) For the two-particle–n-Reggeon vertex [Fig. 10(b)] write a factor $N_{l_1\cdots l_n}$ and use conservation: At the left end of the diagram $\vec{q}_1=\sum\vec{k}_i$, $j_1-1=\sum(l_i-1)$, at the right end $\vec{q}_{n-1}=\sum\vec{k}_i$, $j_{n-1}-1=\sum(l_1-1)$.

(e) There is a factor $V_L(l_1,l_2;k_{1\perp}{}^2,k_{2\perp}{}^2,\eta)$ or $V_R(l_1,l_2;k_{1\perp}{}^2,k_{2\perp}{}^2,\eta)$ for each one-particle–two-Reggeon vertex [Fig. 10(c)]. As indicated, this factor in general depends on momentum and angular momentum of the two attached Reggeons, as well as the η that belongs to the produced particle. The subscript agrees with the corresponding subscript of F: the left-most produced particle with the first subscript of F, etc. In the notation of Fig. 22, the ith produced particle has momentum q_i-q_{i+1} and carries Reggeon energy j_i-j_{i+1}. Correspondingly, there is a conservation law: $\vec{k}_1-\vec{k}_2=(\vec{q}_i-\vec{q}_{i+1})$, $l_1-l_2=(j_i-j_{i+1})$ for this vertex. For a particle–three-Reggeon vertex (Fig. 15), there is another function $W_{L,R}$ together with $\vec{k}_1-\vec{k}_2-\vec{k}_3=(\vec{q}_i-\vec{q}_{i+1})$, $(l_1-1)-(l_2+l_3-1)$

$=(j_i - j_{i+1})$.

(f) For each closed loop there is an integration $\int d^2k_\perp dl/(2\pi)^3 i$. Any diagram is then of the form Fig. 22: To the left of the left-most produced particle total energy and momentum are $j_1 - 1, \tilde{q}_1$, between this and the next-right particle they are $j_2 - 1, \tilde{q}_2$, and so forth. Figure 22 is easily recognized as an n-point function, with the external legs being the $n-2$ produced particles and the right and left end of the diagram. Because of energy and momentum conservation the amplitude depends only on $n-1$ energies and momenta.

(g) Finally, there are still γ factors in the diagram, coming from the combination of signature factors of the internal lines. Since the order in which these signature factors can be combined is not unique, there are different ways to arrange the γ factors. We want to mention one of them. In this case, each vertex $N_{l_1 \cdots l_n}$ and $r_{l_1 - l_m i_1 \cdots l_n}$ with n Reggeons on its right-hand side is accompanied by a factor $\gamma_{l_1 \cdots l_n}$ [defined in (2.28)]. In addition to that, each l integration (see Fig. 22) has a factor $1 = \gamma_{l j_i + 1 - l}/\gamma_{l j_i + 1 - l}$, if the corresponding vertex function has the label L, and a factor $\gamma_{l j_{i+1} + 1 - l}/\gamma_{l j_i + 1 - l}$ when the label is R. The numerators of these factors produce a zero for physical values of j_i and j_{i+1}, and thus ensure that diagrams with cuts decouple from physical angular momentum states. The denominators can always be canceled against other γ factors of the diagram, and their zeros do not produce any poles. Therefore, the diagram has the correct decoupling properties at physical values of angular momentum. But the reason why we have chosen this way of arranging the γ factors is the following one. In practical calculations where one is mainly interested in the region $j_i \sim 1$ and $l_i \sim 0$, the vertices of the diagram are approximated by its value at zero Reggeon momentum and energy, and the γ's are approximated by its value at $l_i = 1$. In the most interesting case, the so-called enhanced diagrams, one has only triple couplings $r_{l_1; l_2 l_3}$ between Reggeons, and the value of $\gamma_{l_2 l_3}$ at $l_i = 1$ is -1. Since there are twice as many vertices $r_{l_1; l_2 l_3}$ as $\gamma_{l_2 l_3}$ in the diagram, one has just a $\sqrt{-1} = i$ for each (real) $r_{l_1; l_2 l_3}$. The γ factors

$$\frac{\gamma_{l j_i + 1 - l}}{\gamma_{l j_i + 1 - l}} \text{ and } \frac{\gamma_{l j_{i+1} + 1 - l}}{\gamma_{l j_i + 1 - l}} ,$$

on the other hand, reduce to 1, and thus the effect of all γ factors together is to make the triple-Reggeon coupling purely imaginary.

We would like to conclude with a few words about the practical use of our Reggeon calculus in production processes. As we have mentioned in our Introduction in paper I, the treatment of the

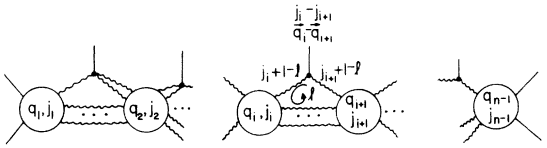

FIG. 22. Typical form of Reggeon diagrams for the $2 \to n$ amplitude.

Pomeron as a simple pole leads to serious theoretical inconsistencies, and it is, therefore, unavoidable to include renormalization effects. In the argument which leads to the unpleasant Pomeron decoupling theorems, the production amplitude plays a crucial role. This motivates a particular interest in a study of the effect of Pomeron cut contributions in the production amplitude. For production processes that allow only Pomeron exchange, such a study has been performed by Migdal, Polyakov, and Ter-Martirosyan.[4] We want to demonstrate how their field theory emerges as an approximation of our Reggeon calculus.

Conventionally, when formulating the Reggeon calculus as a field theory, all vertices are approximated by their value at vanishing external momenta and energies. We have already said that in this approximation the vertex $N_{l_1 l_2}$ and the triple-Reggeon vertex $r_{l_1; l_2 l_3}$, which are real functions, acquire an additional factor i. This comes from the factors $\gamma_{ll'}$, which in our approximation become -1. From our rule (g) it is clear that in any diagram there are just twice as many $N_{ll'}$ and $r_{l;l'l''}$ vertices as $\gamma_{ll'}$ factors, and so there is just one $\sqrt{\gamma} = +i$ for each $N_{ll'}$ and $r_{l;l'l''}$. With the approximation of the vertex functions V_L and V_R one has to be a little careful. When V_R and V_L are approximated by their values at zero Reggeon energy and momentum, then formula (2.17) of paper I teaches us that

$$V_R(\alpha_1 = \alpha_2) = V_L(\alpha_1 = \alpha_2) = V \tag{4.2}$$

and there is no longer any distinction between F_L and F_R: $F_L \equiv F_R \equiv F$. With the further approximations $\eta \sim m^2$ [cf. (2.4)], $\xi_{j_1} \sim \xi_{j_2} \sim -i$, $\xi_{j_1 j_2} \sim 2/\pi(j_1 - j_2) - i$, we then obtain for the $2 \to 3$ amplitude near $j_1 \sim j_2 \sim 1$

$$\left(-\frac{1}{4i}\right)^2 \int dj_1 dj_2 s_{ab}{}^{j_1} s_{bc}{}^{j_2} [\eta^{-j_1} \xi_{j_1} \xi_{j_2 j_1} F_L + \eta^{-j_2} \xi_{j_2} \xi_{j_1 j_2} F_R]$$

$$\sim \left(-\frac{1}{4i}\right)^2 \int dj_1 dj_2 s_{ab}{}^{j_1} s_{bc}{}^{j_2} (m^2)^{-1} (-2F) . \tag{4.3}$$

However, V_R and V_L also contain, in general, higher-order terms:

$$V_R = V_R(\alpha_1 = \alpha_2 = 1) + (\alpha_1 - \alpha_2) V_R'(\alpha_1 = \alpha_2 = 1) + \cdots , \tag{4.4}$$

$$V_L = V_L(\alpha_1 = \alpha_2 = 1) + (\alpha_2 - \alpha_1) V_L'(\alpha_1 = \alpha_2 = 1) + \cdots ,$$

with $V_R' = V_L' = V'$, and when this next leading term is included, (4.3) is modified to

$$\left(\frac{-1}{4i}\right)^2 \int dj_1 dj_2 s_{ab}{}^{j_1} s_{bc}{}^{j_2} (m^2)^{-1} (-2) \left(F + \frac{2i}{\pi} F'\right), \tag{4.5}$$

where F' results from V' and is, in general, not small compared to F. The important result of this is that in (4.5) the coefficient of the energy factors is a complex function: Whereas F_L and F_R are real analytic functions near $j_1 \sim j_2 \sim 1$ and $t_2 \sim t_2 \sim 0$, the amplitude is not pure real or imaginary. This is a consequence of the signature factors.

Formula (4.5) suggests introducing a complex effective coupling constant

$$U = 2\left(V + \frac{2i}{\pi} V'\right) \tag{4.6}$$

for the particle–two-Reggeon vertex, and a factor $-i$ for each subenergy s_{ab} and s_{bc}. It is then not difficult to see that this prescription gives the right structure for the $2 \to 4$ and higher amplitudes near $j_i \sim 1$, $t_1 \sim 0$: instead of being a sum of all the $F_{RL}\ldots$ with their respective signature factors, the $2 \to n$ amplitude has now only one term:

$$T_{2\to n} = \left(-\frac{1}{4i}\right)^{n-1} \int dj_1 \cdots dj_{n-1} (-i)^{n-1} s_{ab}{}^{j_1} \cdots s_{yz}{}^{j_{n-1}} \times (m^2)^{-(n-1)} F(j_1 \cdots j_{n-1};\, t_1 \cdots t_{n-1}), \tag{4.7}$$

where F is a complex-valued function and proportional to U^{n-2}. This leads directly to the field theory of Migdal *et al.*

However, some of the approximations which lead to (4.7) are no longer valid when the quantum numbers of the produced particles allow exchange of other Regge poles. In particular, $V_L = V_R$ is not justified when two different Regge poles couple to the produced particle, and the amplitude remains a sum over several terms with their respective signature factors. The application of our rules to such processes looks rather promising and we hope that our study stimulates further work on these lines.

ACKNOWLEDGMENTS

It is my pleasure to thank H. D. I. Abarbanel, J. B. Bronzan, R. L. Sugar, and A. R. White for encouraging and very helpful discussions.

APPENDIX

We first analyze the diagram of Fig. 23. The blobs contain simple Regge poles, and Fig. 23 is then equivalent to the two-Reggeon diagrams in Fig. 24. The analysis follows closely the pattern of Gribov's original paper, and in our analysis we shall work out only those points which are different from Gribov's discussion.

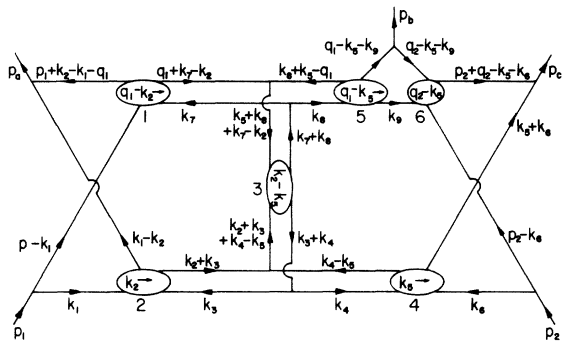

FIG. 23. A hybrid Feynman diagram for the $2 \to 3$ amplitude.

First, we introduce Sudakov variables:

$$\begin{aligned} p_1' &= p_1 - \frac{m^2}{s} p_2, \quad p_2' = p_2 - \frac{m^2}{s} p_1, \\ k_i &= \alpha_i p_2' + \beta_i p_1' + k_{i\perp}, \\ q_1 &= \frac{s_{bc}}{s} p_1' - \frac{q_1^2}{s} p_2' + q_{1\perp}, \\ q_2 &= -\frac{q_2^2}{s} p_1' - \frac{s_{ab}}{s} p_2' + q_{2\perp}. \end{aligned} \tag{A1}$$

The analysis of the crossed box graphs at both sides of the diagram is the same as in the elastic case. It leads to the restrictions

$$\alpha_1 \lesssim \frac{m^2}{s}, \quad \alpha_2 \lesssim \frac{m^2}{s}, \tag{A2}$$

$$\beta_4 \lesssim \frac{m^2}{s}, \quad \beta_5 \lesssim \frac{m^2}{s}. \tag{A3}$$

The momentum transfer along Reggeon 5 is only finite if

$$\alpha_5 \lesssim \frac{m^2}{s_{bc}}. \tag{A4}$$

As a result, we may neglect these parameters in the diagram, wherever they appear in a sum together with other parameters, which are of the order 1. From the link between Reggeon 5 and 6

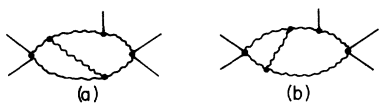

FIG. 24. Reggeon diagrams contained in Fig. 23.

we obtain

$$\alpha_9 \lesssim \frac{m^2}{s_{bc}}\,, \quad \beta_9 \lesssim \frac{m^2}{s_{ab}}\,. \tag{A5}$$

Now we consider the energy of Reggeon 3:

$$(k_3+k_4+k_7+k_8)^2 \sim s[(\alpha_3+\alpha_4)(\beta_7+\beta_8) + (\alpha_7+\alpha_8)(\beta_3+\beta_4)]\,, \tag{A6}$$

where we have already neglected terms of the order $\sim m^2$. (A6) can only be large, if either [case (a)]

$$\alpha_3+\alpha_4 \gg \alpha_7+\alpha_8 \text{ and } \beta_7+\beta_8 \gg \beta_3+\beta_4 \tag{A7a}$$

or [case (b)]

$$\alpha_7+\alpha_8 \gg \alpha_3+\alpha_4 \text{ and } \beta_3+\beta_4 \gg \beta_7+\beta_8\,. \tag{A7b}$$

Since $s\alpha_5\beta_8 \lesssim m^2$ and $s\alpha_5\beta_7 \lesssim m^2$ from the link between Reggeons 1, 3, and 5, we obtain in case (a)

$$\alpha_5 \ll \alpha_3+\alpha_4 \tag{A8}$$

and in a similar way also

$$\beta_2 \ll \beta_7+\beta_8\,. \tag{A9}$$

In case (b)

$$\alpha_5 \ll \alpha_7+\alpha_8 \tag{A8′}$$

$$\beta_2 \ll \beta_3+\beta_4\,. \tag{A9′}$$

From this we obtain the following decoupling scheme for the α_i and β_i integrations ($i=2,5,$): Each of these variables appears in only one vertex (Fig. 25). The vertices are now connected only by the transverse components of k_2, k_5.

Case (a). Next we restrict ourselves to case (a) and look at the Reggeon energies:

Reggeon 1: $(1-\beta_1)\alpha_7 s$; (A10a)

Reggeon 2: $\beta_1\alpha_3 s$; (A10b)

Reggeon 3: $(\alpha_3+\alpha_4)(\beta_7+\beta_8)s$; (A10c)

Reggeon 4: $\beta_4\alpha_6 s$; (A10d)

Reggeon 5: $-\beta_8\alpha_9 s$; (A10e)

Reggeon 6: $(1-\alpha_6)\beta_9 s$. (A10f)

Since (A10a) is to be large, we need $\alpha_7 \gg m^2/s$, but a study of the propagators in the vertex between Reggeons 1, 3, and 5 leads to $\alpha_7 \lesssim m^2/s_{bc}$. Thus,

$$\frac{m^2}{s} \ll \alpha_7 \ll \frac{m^2}{s_{bc}}\,. \tag{A11}$$

Equation (A10e) requires $\beta_8 \gg m^2/s$, but from (A5) we have $\alpha_9 s \lesssim s_{ab}$. Therefore

$$\frac{m^2}{s_{ab}} \ll \beta_8 \ll 1\,. \tag{A12}$$

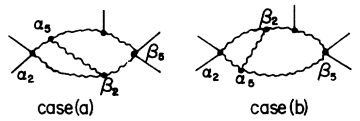

FIG. 25. Distributions of α_2, α_5, β_2, and β_5 integrations in Fig. 23 or 24.

One further shows that the α_8 integration in the vertex 1-3-5 vanishes, if not $|\beta_7| > |\beta_8|$. Thus

$$\frac{m^2}{s_{ab}} \ll \beta_7 \ll 1\,. \tag{A13}$$

All other α_i and β_i in (A10) are in the interval

$$\frac{m^2}{s} \ll \alpha_i,\ \beta_i \ll 1\,. \tag{A14}$$

Using the conditions (A12), (A3), (A8′), (A9), (A12), and (A13), we write down the propagators for the vertex between Reggeons 1, 3, and 5:

$$k_7^2 = s\alpha_7\beta_7 + k_{7\perp}^2\,, \tag{A15a}$$

$$k_8^2 = s\alpha_8\beta_8 + k_{8\perp}^2\,, \tag{A15b}$$

$$(q_1+k_7-k_2)^2 = s\alpha_7\beta_7 + (q_1-k_2+k_7)_\perp^2\,, \tag{A15c}$$

$$(q_1-k_5-k_8)^2 = s(\alpha_5+\alpha_8)\beta_8 + (q_1-k_5-k_8)_\perp^2\,, \tag{A15d}$$

$$(k_7+k_8)^2 = s(\alpha_7+\alpha_8)(\beta_7+\beta_8) + (k_7+k_8)_\perp^2\,, \tag{A15e}$$

$$(k_5+k_7+k_8-k_2)^2 = s(\alpha_5+\alpha_7+\alpha_8)(\beta_7+\beta_8) + (k_5+k_7+k_8-k_2)_\perp^2\,. \tag{A15f}$$

The energy factors from (A10), which belong to this vertex, are

$$\alpha_7^{l_1}, \quad (\beta_7+\beta_8)^{l_3}, \quad (-\beta_8)^{l_5}\,, \tag{A16}$$

with l_i being the angular momentum of the ith Reggeon. From (A15) it follows that for the α_8 (or α_5) integration all singularities lie in the same half plane, and its integration yields zero, if not $\mathrm{sgn}\beta_7 \neq \mathrm{sgn}\beta_8$ and $|\beta_7| > |\beta_8|$. Assuming this, all poles of α_7 coming from the propagators (A15) lie in one half plane, and the α_7 contour can be closed around the energy cut of Reggeon 1 in the opposite half plane. As a result of this, the absorptive part of the amplitude of Reggeon 1 appears. One further shows that the contributions due to the regions $\beta_7>0$, $\beta_8<0$ and $\beta_8>0$, $\beta_7<0$ cancel each other if the signature of Reggeon 1 is different from the product of those of Reggeons 3 and 5. If they are equal, the contributions add up. Now we introduce the variables $\beta_8' = -\beta_8/\beta_7$, $\alpha_5' = -\beta_7\alpha_5$, $\alpha_8' = -\beta_7\alpha_8$, $x = s\alpha_7\beta_7$. Then the expressions in (A15) no longer depend on β_7:

$$k_7^2 = x + k_{7\perp}^2, \tag{A17a}$$

$$k_8^2 = s\alpha_8'\beta_8' + k_{8\perp}^2, \tag{A17b}$$

$$(q_1 + k_7 - k_2)^2 = x + (q_1 - k_2 + k_7)_\perp^2, \tag{A17c}$$

$$(q_1 - k_5 - k_8)^2 = s(\alpha_5' + \alpha_8')\beta_8' + (q_1 - k_5 - k_8)_\perp^2, \tag{A17d}$$

$$(k_7 + k_8)^2 = x(1 - \beta_8') + s\alpha_8'(1 - \beta_8') + (k_7 + k_8)_\perp^2, \tag{A17e}$$

$$(k_5 + k_7 + k_8 - k_2)^2 = x(1 - \beta_8') + s(\alpha_5' + \alpha_8')(1 - \beta_8') + (k_5 + k_7 + k_8 - k_2)_\perp^2, \tag{A17f}$$

and the β_7 integration can be done explicitly. We obtain for this vertex

$$\begin{aligned}
&\text{const} \times s^2 \int d^2k_7 d^2k_8 \int d\alpha_5 d\alpha_7 d\beta_7 d\alpha_8 d\beta_8\, \alpha_7^{l_1}(\beta_7+\beta_8)^{l_3}\beta_8^{l_5}\, ggg \frac{1}{k_7^2 - m^2} \\
&\qquad \times \frac{1}{(q_1+k_7-k_2)^2 - m^2} \frac{1}{k_8^2 - m^2} \frac{1}{(k_8+k_5-q_1)^2 - m^2} \frac{1}{(k_7+k_8)^2 - m^2} \frac{1}{(k_5+k_7+k_8-k_2)^2 - m^2} \\
&= \text{const} \times s^{-l_1-1} \int_{m^2/s_{ab}}^1 d\beta_7 \beta_7^{l_3+l_5-l_1-2} s^2 \int d^2k_7 d^2k_8 \int dx\, d\alpha_5' d\alpha_8' d\beta_8' x^{l_1}(1-\beta_8')^{l_3}(\beta_8')^{l_5}\, ggg \times \text{propagators} \\
&= s^{-l_1-1} \frac{1 - (1/s_{ab})^{l_3+l_5-l_1-1}}{l_3 + l_5 - l_1 - 1} r_{l_1; l_3 l_5},
\end{aligned} \tag{A18}$$

where $r_{l_1; l_3 l_5}$ is the same function for the three-Reggeon coupling as in Gribov's original paper, being independent of the energies.

For the vertex between Reggeons 2, 3, and 4, the analysis proceeds in the same way, except for the fact that s_{ab} does not appear:

$$\frac{m^2}{s} \ll \alpha_3 \ll 1, \tag{A19}$$

$$\frac{m^2}{s} \ll \alpha_4 \ll 1, \tag{A20}$$

$$\frac{m^2}{s} \ll \beta_4 \ll 1. \tag{A21}$$

These conditions are the analog of (A11)–(A13). The result of the analysis ($d\alpha_1$, d^4k_3, d^4k_4 integrations) is

$$s^{-l_4-1} \frac{1 - (1/s)^{l_3+l_2-l_4-1}}{l_3 + l_2 - l_4 - 1} r_{l_4; l_2 l_3}. \tag{A22}$$

Finally, we have to analyze the link between Reggeons 5 and 6. This is done in Ref. 10 and we quote only the result:

$$\begin{aligned}
&\xi_{l_5}\xi_{l_6} \times \text{const} \times \int d\alpha_9 d\beta_9 d^2k_\perp (\beta_9 s)^{l_6} (\alpha_9 s)^{l_5} gg \frac{1}{k_9^2 - m^2} \frac{1}{(q_1 - k_5 - k_9)^2 - m^2} \frac{1}{(q_2 - k_2 - k_9)^2 - m^2} \\
&= s_{ab}^{l_5} s_{bc}^{l_6} f_{l_5 l_6}((q_1-k)_\perp^2, (q_2-k)_\perp^2, \eta)\, \xi_{l_5}\xi_{l_6 l_5} \\
&= s_{ab}^{l_5} s_{bc}^{l_6} [\eta^{-l_5} V_L(l_5, l_6; (q_1-k)_\perp^2, (q_2-k)_\perp^2, \eta)\, \xi_{l_5}\xi_{l_6 l_5} + \eta^{-l_6} V_R(l_5, l_6; (q_1-k)_\perp^2, (q_2-k)_\perp^2, \eta)\, \xi_{l_6}\xi_{l_5 l_6}].
\end{aligned} \tag{A23}$$

Now we are in the position to combine all energy factors: With the introduction of Sudakov variables: $d^4k_i = (\frac{1}{2}|s|)\, d\alpha_i\, d\beta_i\, dk_{i\perp}$ we obtain, in addition to the Reggeon energies, s^9; but a factor s^2 is necessary for each of the two N's and the r's to make them energy-independent, and a factor s is necessary for $f_{l_5 l_6}$. We are then left with

$$s^{l_1} s^{l_2} s^{l_3} s_{ab}^{l_5} s_{bc}^{l_6} s^{l_4} s^{-l_4-1} \frac{1 - (1/s)^{l_3+l_2-l_4-1}}{l_3 + l_2 - l_4 - 1} s^{-l_1-1} \frac{1 - (1/s_{ab})^{l_3+l_5-l_1-1}}{l_3 + l_5 - l_1 - 1}. \tag{A24}$$

Expressing s through (2.2) in terms of η, s_{ab}, and s_{bc} and taking the double Mellin transform with respect to s_{ab} and s_{bc}, we obtain

$$\eta\frac{1}{l_4-(l_2+l_3-1)}\left[\eta^{-l_4}\frac{1}{j_2-(l_4+l_6-1)}\frac{1}{j_1-(l_4+l_5-1)}\frac{1}{j_1+l_3+l_4-l_1}\right.$$
$$\left.-\eta^{-(l_3+l_2+1)}\frac{1}{j_2-(l_2+l_3+l_6-2)}\frac{1}{j_1-(l_2+l_3+l_5-2)}\frac{1}{j_1-(l_1+l_2-1)}\right]. \quad \text{(A25)}$$

Making use of the fact that $\mathrm{Re}j_1>\mathrm{Re}l_i$ and $\mathrm{Re}j_2>\mathrm{Re}l_i$, we can do some of the l_i integration and convince ourselves that (A25) is equivalent to

$$\eta^{-(l_4-1)}(2\pi i)^4\delta(j_2-(l_4+l_6-1))\,\delta(j_1-(l_1+l_2-1))$$
$$\times\delta(l_4-(l_2+l_3-1))\,\delta(l_1-(l_2+l_3-1)). \quad \text{(A26)}$$

Finally, we have to take care of the signature factors. We observe that for Reggeons 1 and 4 only the absorptive part of the subamplitude enters into the whole amplitude, and we are then left with ξ_{l_2}, ξ_{l_3} and the signature factors in (A23). For the first part in the brackets in (A23), we use (2.11) and combine ξ_{l_3} with ξ_{l_5} to $i\gamma_{l_3l_5}\xi_{l_1}$ and this with ξ_{l_2} to

$$\xi_{l_2}\xi_{l_3}\xi_{l_5}\xi_{l_6l_5}=i\gamma_{l_1l_2}i\gamma_{l_3l_5}\xi_{l_1+l_2-1}\xi_{l_6l_5}$$
$$=i\gamma_{l_1l_2}i\gamma_{l_3l_5}\xi_{j_1}\xi_{j_2j_1}. \quad \text{(A27)}$$

In the second part of (A24) we arrange the signature factors in the following way:

$$\xi_{l_2}\xi_{l_3}\xi_{l_6}\xi_{l_5l_6}=i\gamma_{l_3l_5}i\gamma_{l_1l_2}\frac{i\gamma_{l_4l_6}}{i\gamma_{l_4l_5}}\xi_{j_2}\xi_{j_1j_2}. \quad \text{(A28)}$$

Instead of this, we could have combined in another way

$$\xi_{l_2}\xi_{l_3}\xi_{l_5}\xi_{l_6l_5}=i\gamma_{l_2l_3}i\gamma_{l_4l_5}\xi_{j_1}\xi_{j_2j_1},$$
$$\xi_{l_2}\xi_{l_3}\xi_{l_6}\xi_{l_5l_6}=i\gamma_{l_2l_3}i\gamma_{l_4l_6}\xi_{j_2}\xi_{j_1j_2}. \quad \text{(A29)}$$

There we see explicitly the factors $\gamma_{l_4l_5}$ and $\gamma_{l_4l_6}$ which generate zeros when j_1 and j_2 take physical values. It is also clear from (A29) that there are no poles from zeros of γ, as it might seem from (A28). The form (A27), (A28), however, yields explicitly a γ factor for each vertex with two leaving Reggeons ($N_{l_1l_2}$ and $r_{l_1;\,l_3l_5}$ in our case), and one can see fairly easily that this holds for any diagram. But in all considered diagrams we found it possible to arrange the signature factors similarly to (A29), i.e., without denominators of γ factors. Returning to (A27), (A28), we combine them and obtain

$$\eta^{-(l_4-1)}\xi_{l_2}\xi_{l_3}(\eta^{-l_5}V_L\xi_{l_5}\xi_{l_6l_5}+\eta^{-l_6}V_R\xi_{l_6}\xi_{l_5l_6})$$
$$=\eta^{-j_1}\xi_{j_1}\xi_{j_2j_1}i\gamma_{l_1l_2}i\gamma_{l_3l_5}V_L$$
$$+\eta^{-j_2}\xi_{j_2}\xi_{j_1j_2}i\gamma_{l_1l_2}i\gamma_{l_3l_5}\frac{i\gamma_{l_4l_6}}{i\gamma_{l_5l_6}}V_R. \quad \text{(A30)}$$

Thus our final result for our diagram Fig. 24(a) is of the form (2.6), with

$$F_{\{L,R\}}=\int\frac{dl_1\cdots dl_6}{(2\pi i)^6}\int\frac{d^2k_2d^2k_5}{(2\pi)^4}(2\pi i)^4\delta(j_1-(l_1+l_2-1))\delta(j_2-(l_4+l_6-1))$$
$$\times\delta(l_4-(l_2+l_3-1))\delta(l_1-(l_2+l_3-1))N_{l_1l_2}\gamma_{l_1l_2}N_{l_4l_6}$$
$$\times r_{l_1;\,l_3l_5}\gamma_{l_3l_5}r_{l_4;\,l_2l_3}V_{\{L,R\}}(l_5,\,l_6;\,(q_1-k_5)_\perp^2,\,(q_2-k_5)_\perp^2,\,\eta)$$
$$\times G_{l_1}((q_1-k_2)_\perp^2)\,G_{l_2}(k_{2\perp}^2)G_{l_3}((k_2-k_5)_\perp^2)G_{l_4}(k_{5\perp}^2)G_{l_5}((q_1-k_5)_\perp^2)G_{l_6}((q_2-k_5)_\perp^2)\left\{1,\frac{\gamma_{l_4l_6}}{\gamma_{l_4l_5}}\right\}. \quad \text{(A31)}$$

Case (b). The Reggeon energies remain unchanged, except for Reggeon 3:

$$(\alpha_7+\alpha_8)(\beta_3+\beta_4)s \quad \text{(A32)}$$

instead of (A10c). Equations (A11) and (A12) are still valid, and the requirement that there must be poles for β_7 in both half planes demands $|\alpha_8|>|\alpha_7|$. On the other hand, we have $s_{bc}\alpha_8\lesssim m^2$ from the propagator $(q_1-k_5-k_8)^2-m^2$:

$$\frac{m^2}{s}\ll|\alpha_8|\ll\frac{m^2}{s_{bc}}. \quad \text{(A33)}$$

Now we proceed in the same way as in case (a): For the vertex 1-3-5, the energy factors are

$$\alpha_7^{l_1}(\alpha_7+\alpha_8)^{l_3}\beta_8^{l_5}. \quad \text{(A34)}$$

The β_8 integration becomes an integral over the absorptive part of Reggeon 5, and by change of variables, $\alpha_7'=-\alpha_7/\alpha_8$, $\beta_2'=-\alpha_8\beta_2$, $\beta_7=-\alpha_8\beta_7'$, $x=s\alpha_8\beta_8$, we can do the β_8 integration. The result is

$$s^{-(l_1+l_3-1)-1}\frac{1-(1/s_{ab})^{l_5-(l_1+l_3-1)}}{l_5-(l_1+l_3-1)}r_{l_5;\,l_1l_3}. \quad \text{(A35)}$$

Together with

$$s^{-l_4}\,\frac{1-(1/s)^{l_2+l_3-1-l_4}}{l_2+l_3-1-l_4}\,\gamma_{l_4;\,l_2 l_3} \tag{A36}$$

for the lower three-Reggeon vertex we obtain for the double Mellin transform

$$\frac{1}{l_3+l_4-1-l_2}\left[\eta^{-(l_4-1)}\,\frac{1}{j_2-(l_4+l_6-1)}\,\frac{1}{j_1-(l_4+l_5-1)}\,\frac{1}{j_1-(l_1+l_3+l_4-2)}\right.$$
$$\left.-\eta^{-(l_2-l_3)}\,\frac{1}{j_2-(l_6+l_2-l_3)}\,\frac{1}{j_1-(l_2+l_5-l_3)}\,\frac{1}{j_1-(l_1+l_2-2l_3-1)}\right], \tag{A37}$$

which is equivalent to

$$\eta^{-(l_4-1)}(2\pi i)^4\delta(j_1-(l_4+l_5-1))\delta(j_2-(l_4+l_6-1))\delta(l_3+l_4-1-l_2)\delta(l_1+l_3-1-l_5)\,. \tag{A38}$$

As to the signature factors, we combine ξ_{l_1} and ξ_{l_3} with ξ_{l_5} and obtain

$$i\gamma_{l_1 l_3}\xi_{l_5}f_{l_5 l_6}\xi_{l_6}\xi_{l_4} = i\gamma_{l_1 l_3}(i\gamma_{l_4 l_5}\xi_{l_4+l_5-1}\xi_{l_6 l_5}\eta^{-l_5}V_L + i\gamma_{l_4 l_6}\xi_{l_4+l_6-1}\xi_{l_5 l_6}\eta^{-l_6}V_R) \tag{A39}$$

or

$$i\gamma_{l_1 l_2}\,i\gamma_{l_3 l_4}\left[\xi_{j_1}\xi_{j_2 j_1}\eta^{-l_5}V_L + \frac{i\gamma_{l_4 l_6}}{i\gamma_{l_4 l_5}}\,\xi_{j_2}\xi_{j_1 j_2}\eta^{-l_6}V_R\right]\,. \tag{A40}$$

With this we again arrive at (2.6), with

$$F_{\{L,R\}} = \int\frac{dl_1\cdots dl_6}{(2\pi i)^6}\int\frac{d^2k_2 d^2k_5}{(2\pi)^4}\,(2\pi i)^4\delta(j_1-(l_1+l_2-1))\delta(j_2-(l_4+l_6-1))$$
$$\times\delta(l_2-(l_3+l_4-1))\delta(l_5-(l_1+l_3-1))\,N_{l_1 l_2}\gamma_{l_1 l_2}N_{l_4 l_6}\gamma_{l_5;\,l_1 l_3}\gamma_{l_2;\,l_3 l_4}$$
$$\times\gamma_{l_3 l_4}V_{\{L,R\}}(l_5,\,l_6,\,(q_1-k_5)_\perp^2,\,(q_2-k_5)_\perp^2,\,\eta)G_{l_1}((q_1-k_2)_\perp^2)G_{l_2}(k_{2\perp}^2)G_{l_3}((k_2-k_5)_\perp^2)$$
$$\times G_{l_4}(k_{5\perp}^2)G_{l_5}((q_1-k_5)_\perp^2)G_{l_6}((q_2-k_5)_\perp^2)\left\{1,\ \frac{\gamma_{l_6 l_4}}{\gamma_{l_5 l_4}}\right\}\,. \tag{A41}$$

Finally, we consider diagram Fig. 26. From the requirement that the energy of the subamplitude 3,

$$s(\alpha_3+\alpha_4)(\beta_7+\beta_8)+s(\alpha_7+\alpha_8)(\beta_3+\beta_4), \tag{A42}$$

has to be large, we obtain again the two cases (A7a) and (A7b) together with (A8) and (A9). They correspond to the Reggeon diagrams in Figs. 27(a) and 27(b). In case (a), the upper three-Reggeon vertex depends only on α_5, and the lower one on β_2. Determining the intervals for the α, β parameters which appear in the Reggeon energies in the same way as for the previous diagram, we obtain for the upper vertex

$$s^{-l_1-1}\,\frac{1-(1/s_{ab})^{l_3+l_5-1-l_1}}{l_3+l_5-1-l_1}\,\gamma_{l_1;\,l_3 l_5} \tag{A43}$$

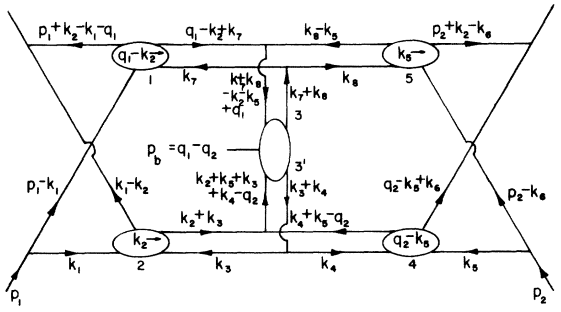

FIG. 26. Another hybrid Feynman diagram for the 2→3 amplitude.

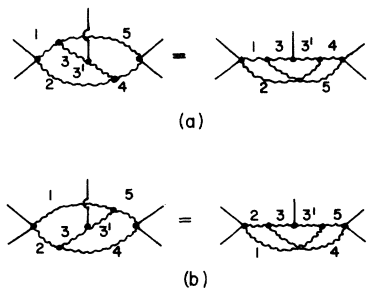

FIG. 27. Reggeon diagrams obtained from Fig. 26.

and for the lower one (by symmetry arguments)

$$s^{-l_4-1}\,\frac{1-(1/s_{bc})^{l_2+l_3'-1-l_4}}{l_2+l_3'-1-l_4}\,\gamma_{l_4;\,l_2 l_3'}\,. \tag{A44}$$

Combining all s factors, reexpressing s in terms of s_{ab}, s_{bc} and η and taking the double Mellin transform with respect to s_{ab}, s_{bc}, we obtain

$$\left(\frac{1}{\eta}\right)^{l_2+l_5-2}\frac{1}{j_1-(l_2+l_3+l_5-2)}\,\frac{1}{j_1-(l_1+l_2-1)} \times\frac{1}{j_2-(l_2+l_3'+l_5-2)}\,\frac{1}{j_2-(l_4+l_5-1)}\,, \tag{A45}$$

which is equivalent to

$$\left(\frac{1}{\eta}\right)^{l_2+l_5-2}(2\pi i)^4\delta(j_1-(l_1+l_2-1))\delta(j_2-(l_4+l_5-1)) \times\delta(l_1-(l_3+l_5-1))\delta(l_4-(l_2+l_3'-1))\,. \tag{A46}$$

The exponent of η is the sum of angular momentum, carried by the Reggeon under the produced particle (see Fig. 22), and together with the η factors η^{-l_3}, $\eta^{-l_3'}$ from the vertex of the produced particle the η factors become

$$\eta^{-l_3}\left(\frac{1}{\eta}\right)^{l_2+l_5-2}=\eta^{-j_1},\quad \eta^{-l_3'}\left(\frac{1}{\eta}\right)^{l_2+l_5-2}=\eta^{-j_2}\,. \tag{A47}$$

The signature factors: $\xi_{l_2}\xi_{l_5}\xi_{l_3}f_{l_3 l_3'}\xi_{l_3'}$ are shown to be

$$i\gamma_{l_1 l_2}\,i\gamma_{l_3 l_5}\left(\eta^{-l_3}\xi_{j_1}\xi_{j_2 j_1}V_L + \eta^{-l_3'}\,\frac{i\gamma_{l_3',\,l_2+l_5-1}}{i\gamma_{l_3,\,l_2+l_5-1}}\,\xi_{j_2}\xi_{j_1 j_2}V_R\right), \tag{A48}$$

and our expressions for $F_{L,R}$ become

$$F_{\{L,R\}}=\int\frac{d^2k_2\,d^2k_5}{(2\pi)^4}\int\frac{dl_1\cdots dl_5}{(2\pi i)^6}(2\pi i)^4\delta(j_1-(l_1+l_2-1))\delta(j_2-(l_4+l_5-1))\delta(j_2-(l_4+l_4-1))\delta(l_1-(l_3+l_5-1)) \times N_{l_1 l_2}\gamma_{l_1 l_2}N_{l_4 l_5}\gamma_{l_i;\,l_3 l_5}\gamma_{l_3 l_5}\gamma_{l_4;\,l_2 l_3'}G_{l_1}G_{l_2}G_{l_3}G_{l_3'}G_{l_4}G_{l_5} \times V_{\{L,R\}}(l_3,l_3',(q_1-k_2-k_5)_\perp^2,(q_2-k_2-k_5)_\perp^2,\eta)\left\{1,\frac{\gamma_{l_3',l_3+l_5-1}}{\gamma_{l_3,l_3+l_5-1}}\right\}\,. \tag{A49}$$

The remaining case (b) leads to the same expression.

*Work supported by the Max Kade Foundation.
†Operated by Universities Research Association Inc. under contract with the United States Atomic Energy Commission.

[1]J. Bartels, preceding paper, Phys. Rev. D 11, 2977 (1975).
[2]V. N. Gribov, Zh. Eksp. Teor. Fiz. 53, 654 (1967) [Sov. Phys.—JETP 26, 414 (1968)].
[3]H. D. I. Abarbanel and J. B. Bronzan, Phys. Rev. D 9, 2397 (1974); H. D. I. Abarbanel and R. L. Sugar, *ibid.* 10, 721 (1974); R. Savit and J. Bartels, *ibid.* 11, 2300 (1975).
[4]A. A. Migdal, A. M. Polyakov, and K. A. Ter-Martirosyan, Moscow Report No. ITEP-102 (unpublished); Phys. Lett. 48B, 239 (1974).
[5]I. T. Drummond, Phys. Rev. 176, 2003 (1968).
[6]D. K. Campbell, Phys. Rev. 188, 2471 (1969).
[7]We use formula (52) of Ref. 5, but instead of $\xi_{l_1}f_{l_1 l_2}\xi_{l_2}$ there we write our bracket term. We mentioned in Sec. I that the factorized form and the decomposition of the $2\to 3$ amplitude are equivalent.
[8]J. Bartels, unpublished.
[9]A. R. White, private communication, and unpublished work.
[10]We refer to formula (51) of Ref. 6. Our bracket term is the same as $\xi_{l_1}f_{l_1 l_2}\xi_{l_2}f_{l_2 l_3}\xi_{l_3}$ in Ref. 6.
[11]It is formula (78) of Ref. 11 with our two bracket terms in place of $\xi_{\alpha_1}f_{\alpha_1\alpha_2}\xi_{\alpha_2}$ and $\xi_{\alpha_1'}f_{\alpha_2'\alpha_2'}\xi_{\alpha_2'}$.